THE JOURNAL OF CELL BIOLOGY

Katsuhisa Matsuura, Hiroshi Wada, Toshio Nagai, Yoshihiro Iijima, Tohru Minamino, Masanori Sano, Hiroshi Akazawa, Jeffery D. Molkentin, Hiroshi Kasanuki, and Issei Komuro

Vol. 167, No. 2, October 25, 2004. Pages 351–363.

A label (RFP$^+$ HUVEC) was left out of figure 2 B. The corrected figure appears below.

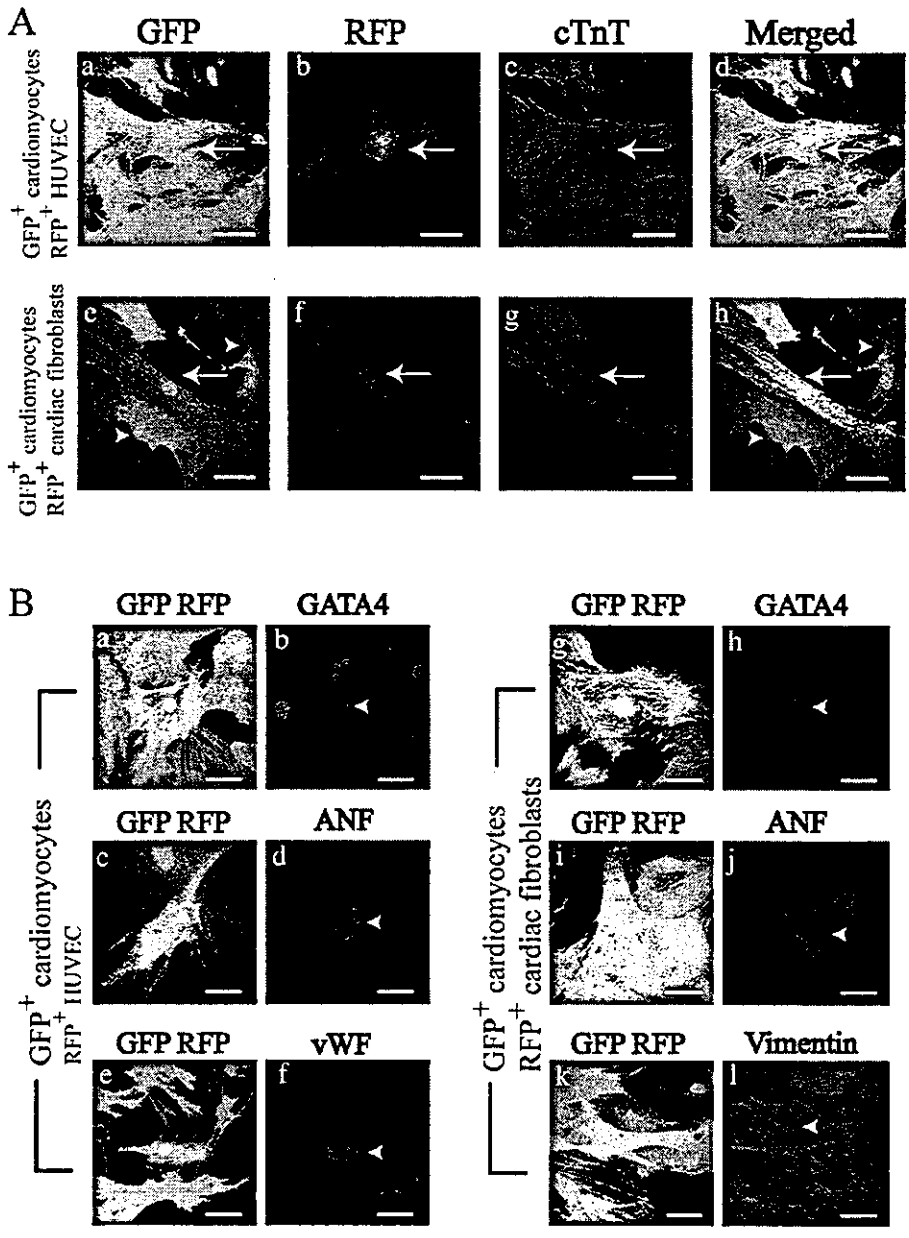

THE JOURNAL OF BIOLOGICAL CHEMISTRY
Vol. 279, No. 39, Issue of September 24, pp. 41095–41103, 2004
Printed in U.S.A.

Diphtheria Toxin-induced Autophagic Cardiomyocyte Death Plays a Pathogenic Role in Mouse Model of Heart Failure*

Received for publication, December 1, 2003, and in revised form, May 20, 2004
Published, JBC Papers in Press, July 22, 2004, DOI 10.1074/jbc.M313084200

Hiroshi Akazawa‡§, Shinji Komazaki¶, Hiroaki Shimomura‖, Fumio Terasaki‖, Yunzeng Zou‡, Hiroyuki Takano‡, Toshio Nagai‡, and Issei Komuro‡**

From the ‡Department of Cardiovascular Science and Medicine, Chiba University Graduate School of Medicine, 1-8-1 Inohana, Chuo-ku, Chiba 260-8670, Japan, the ¶Department of Anatomy, Saitama Medical School, 38 Morohongou, Moroyama, Iruma 350-0495, Japan, ‖The Third Division, Department of Internal Medicine, Osaka Medical College, 2-7 Daigaku-machi, Takatsuki 569-8686, Japan, and the §Foundation for Biomedical Research and Innovation, 6-1, Minatojima Nakamachi, Chuo-ku, Kobe 650-8543, Japan

It is still not clear whether loss of cardiomyocytes through programmed cell death causes heart failure. To clarify the role of cell death in heart failure, we generated transgenic mice (TG) that express human diphtheria toxin receptor in the hearts. A mosaic expression pattern of the transgene was observed, and the transgene-expressing cardiomyocytes (17.3% of the total cardiomyocytes) were diffusely scattered throughout the ventricles. Intramuscular injection of diphtheria toxin induced complete elimination of the transgene-expressing cardiomyocytes within 7 days, and ~80% of TG showed pathophysiological features characteristic of heart failure and were dead within 14 days. Degenerated cardiomyocytes of the TG heart showed characteristic features indicative of autophagic cell death such as up-regulated lysosomal markers and abundant autophagosomes containing cytosolic organelles like cardiomyocytes of human dilated cardiomyopathy. The heart failure-inducible TG are a useful model for dilated cardiomyopathy, and provided evidence indicating that myocardial cell loss through autophagic cell death plays a causal role in the pathogenesis of heart failure.

Cardiomyocyte death is observed in a number of pathological conditions such as ischemic or dilated cardiomyopathy, hypertensive heart disease, and aging (1). Oncosis has been recognized to be a principal mechanism of myocardial cell death, but during the last decade, much emphasis has been put on the importance of apoptosis on the basis of detectable apoptotic cardiomyocytes in animal and human models of heart failure (2). Recently, autophagic cell death (ACD)[1] has been demonstrated as another type of myocardial cell death in human failing hearts (3–7). Although a decline in pumping capacity initiated by cardiomyocyte loss is supposed to induce ventricular remodeling and finally results in symptomatic heart failure (8), there still remains a controversy over the pathogenic role of cell death in progression of heart failure (9, 10). An intractable problem that hampers mechanistic insights is the low occurrence of myocardial cell death in failing hearts, although it differs strikingly according to the models examined and technical specificity (2, 8). Furthermore, in human hearts, most samples were obtained from patients with end-stage heart failure who underwent heart transplantation and thus it remains unknown whether myocardial cell death occurs persistently from an early stage and is causative to progression of heart failure (8). To circumvent these obstacles, we established an inducible heart failure mouse model utilizing diphtheria toxin (DT)-mediated cell ablation, in which a given number of cardiomyocytes are arbitrarily and synchronously ablated, and prospective and serial analysis is available.

DT is a two-peptide protein consisting of fragments A (DT-A) and B (DT-B) produced by *Corynebacterium diphtheriae* (11). DT binds to the DT receptor on the cell surface through DT-B and is internalized into acidic endocytic vesicles, which allows release of catalytic DT-A into the cytoplasm (12). DT-A exerts its cytotoxicity by ADP-ribosylating elongation factor 2 and thereby inhibiting protein synthesis in infected cells (13). DT receptor has been identified as a precursor of heparin-binding EGF-like growth factor (pro-HB-EGF) (14, 15). Intriguingly, DT cannot bind to rodent pro-HB-EGF because of substitution of amino acids required for DT binding, whereas primate pro-HB-EGF acts as a functional DT receptor (16). Therefore, specific cells in mice are ideally sensitized to DT by forced expression of human pro-HB-EGF (17).

To enable cardiac-specific cell ablation, we generated transgenic mice (TG) expressing human pro-HB-EGF in the hearts under the control of *α-myosin heavy chain* promoter. Administration of DT induced ablation of transgene-expressing cardiomyocytes, and subsequently symptomatic heart failure. In this mouse model of heart failure, autophagy but not apoptosis was the mechanism of cardiomyocyte death. Autophagy is a dynamic process and intracellular constituents are sequestered by membranes and subsequently degradated or recycled in lysosome or vacuole (18–20). In this sense, autophagy is involved in maintaining cellular homeostasis and turnover in physiological conditions. However, a growing body of evidence suggests that autophagy is implicated in execution of pro-

* This work was supported in part by grants from the Japanese Ministry of Education, Science, Sports, and Culture of Japan, Japan Health Sciences Foundation, Takeda Medical Research Foundation, Takeda Science Foundation, Uehara Memorial Foundation, Kato Memorial Trust for Nambyo Research, an the Japan Medical Association (to I. K.) and a Japanese Heart Foundation/Pfizer Japan Grant on Cardiovascular Disease Research (to H. A.), and the New Energy and Industrial Technology Development Organization. The costs of publication of this article were defrayed in part by the payment of page charges. This article must therefore be hereby marked "*advertisement*" in accordance with 18 U.S.C. Section 1734 solely to indicate this fact.

** To whom correspondence should be addressed. Tel.: 81-43-226-2097; Fax: 81-43-226-2557; E mail: komuro-tky@umin.ac.jp.

[1] The abbreviations used are: ACD, autophagic cell death; BNP, brain natriuretic peptide; DT, diphtheria toxin; DT-A, DT fragment A; DT-B, DT fragment B; LAMP-1, lysosome-associated membrane protein-1; MCP-1, macrophage chemoattractant protein-1; MLP, muscle LIM protein; pro-HB-EGF, precursor of heparin-binding epidermal growth factor-like growth factor; SERCA2, sarcoplasmic reticulum calcium-ATPase 2; TG, transgenic mice; WT, wild-type mice.

grammed cell death and is closely linked to several pathological conditions (21–23). Our model of experimentally induced heart failure provided direct evidence that myocardial cell loss through ACD causes heart failure, and will be useful to dissect the molecular mechanisms underlying structural and functional changes in heart failure.

EXPERIMENTAL PROCEDURES

Generation of Transgenic Mice—Human *pro-HB-EGF* cDNA (gift from A. Ullrich, Max-Planck-Institute of Biochemistry, Martinsried, Germany) was subcloned into the α-myosin heavy chain promoter-containing expression vector (gift from J. Robbins, Children's Hospital, Cincinnati, OH). The 6.9-kb DNA fragment was microinjected as a transgene into pronuclei of eggs from BDF1 mice, and the eggs were transferred into the oviducts of pseudopregnant ICR mice. The transgene was identified by Southern blot and PCR analysis. All protocols using mice were approved by the Institutional Animal Care and Use Committee of Chiba University.

Administration of Diphtheria Toxin—Diphtheria toxin (Sigma) was reconstituted in 10 mM sodium phosphate buffer (pH 7.4) containing 5% lactose, and was administered by intramuscular injection.

Northern Blot and in Situ Hybridization Analysis—For Northern blot analysis, total RNA (20 μg) prepared from tissues were hybridized with cDNA probes. Probes for brain natriuretic peptide (*BNP*), skeletal α-actin, sarcoplasmic reticulum calcium-ATPase 2 (*SERCA2*), and *TNF-α* were previously described (24–26). Probes for macrophage chemoattractant protein-1 (*MCP-1*) and collagens (*Col1a2* and *Col3a1*) were gifts from K. Matsushima (Universitty of Tokyo, Tokyo, Japan) and S. Kim (Osaka City University, Osaka, Japan), respectively. Digoxygenin-labeled riboprobes were synthesized by using the 0.7-kb human *pro-HB-EGF* cDNA, and RNA *in situ* hybridization was performed as described previously (27).

Western Blot Analysis—Protein samples were fractionated by SDS-PAGE, and immunoblot analysis was performed as described previously (26, 28).

Transthoracic Echocardiography—Mice were anesthetized by intraperitoneal injection of a mixture of ketamine (100 mg/kg) and xylazine (5 mg/kg). Cardiac function was evaluated with echocardiography (SONOS 4500, Philips, Eindhoven, the Netherlands) using a 12-MHz transducer as described previously (26).

Histological Analysis and Immunohistochemistry—Hearts were fixed in 10% neutralized formalin and embedded in paraffin. Serial sections at 5 μm were routinely stained with hematoxylin-eosin for morphological analysis, and with Masson's trichrome for detection of fibrosis. For measurement of the myocyte cross-sectional area, semithin sections with silver staining were analyzed. Suitable cross-sections were defined as having round-to-oval cardiomyocyte sections and nearly round-shaped capillaries that perfused in the region. For immunohistochemistry, Vectastain ABC kit (Vector Laboratories, Burlingame, CA) was used to detect the primary antibodies. The sections were counterstained with hematoxylin.

Antibodies—The following antibodies were used: goat polyclonal anti-human HB-EGF (R&D Systems, Minneapolis, MN), anti-actin (20–33) IgG fraction of antiserum developed in rabbit (Sigma), mouse monoclonal anti-Ly-6G, mouse monoclonal anti-Mac-3, mouse monoclonal anti-CD3, mouse monoclonal anti-Bcl-xL, mouse monoclonal anti-cytochrome *c* (BD Pharmingen, San Diego, CA), rabbit polyclonal anti-caspase 3, mouse monoclonal anti-phospho-Bad, rabbit polyclonal anti-Bad (Cell Signaling, Beverly, MA), rabbit polyclonal anti-Bcl2, rabbit polyclonal anti-Bax, goat polyclonal anti-cathepsin D, rat monoclonal anti-lysosome-associated membrane protein-1 (LAMP-1), goat polyclonal anti-UBC2, goat polyclonal anti-E6-AP, goat polyclonal anti-UFD1 (Santa Cruz Biotechnology, Santa Cruz, CA), mouse monoclonal anti-COX I (Molecular Probes, Eugene, OR), mouse monoclonal anti-ubiquitin (Chemicon, Temecula, CA), and mouse monoclonal anti-E1 (Upstate, Charlottesville, VA).

Evaluation of DNA Fragmentation—TUNEL assay using paraffin sections was performed with an *in situ* apoptosis detection kit (Takara Biomedicals, Otsu, Japan). For agarose gel electrophoresis for DNA fragmentation, genome DNA (10 μg) was electrophoretically fractionated on a 1.5% agarose gel and stained with ethidium bromide as described previously (29). To induce apoptosis in spleens as positive controls, we injected lipopolysaccharide (40 mg/kg) (Sigma) in phosphate-buffered saline intraperitoneally into age-matched mice. Mice were sacrificed 12 h after lipopolysaccharide injection and spleens were excised (30).

Electronmicroscopy—Hearts were fixed in 3% paraformaldehyde, 2.5% glutaraldehyde, and 0.1 M cacodylate buffer (pH 7.4). After washing with the buffer solution and post-fixation in 1% OsO_4 and 0.1 M cacodylate buffer (pH 7.4), they were washed with the buffer solution, dehydrated using alcohol and acetone, and embedded in epoxy resin. Ultrathin sections were examined under the electron microscope (31).

Statistical Analysis—All values are expressed as mean ± S.E. Comparisons were made by Student's *t* test or one-way analysis of variance as appropriate. Values of $p < 0.05$ were considered statistically significant.

RESULTS

Inducible Myocardial Cell Ablation in TG Expressing Human DT Receptor in the Hearts—To confer DT sensitivity to cardiomyocytes in mice, we generated TG expressing human DT receptor, pro-HB-EGF, under the control of the α-myosin heavy chain promoter (Fig. 1*A*). Of two independent founder lines with successful germline transmission, one line was chosen for further analysis on the basis of transgene expression levels. By immunoblot analysis using an antibody specific for human pro-HB-EGF, we confirmed cardiac-specific expression of the transgene (Fig. 1*B*). *In situ* hybridization analysis using a specific riboprobe for human *pro-HB-EGF* further revealed a mosaic expression pattern of the transgene in the hearts (Fig. 1*C*). Expression of the transgene was scattered throughout the TG hearts, and the number of transgene-expressing cardiomyocytes was 17.3 ± 6.0% out of total cardiomyocytes.

To induce DT-mediated myocardial cell ablation, we administered DT by intramuscular injection to TG and wild-type mice (WT) at 10 weeks of age. When 5 mg/kg DT was administered, TG became lethargic and ~80% of TG died within 10 days after injection of DT, although WT appeared normal (Fig. 1*D*). Immunoblot analysis in combination with *in situ* hybridization analysis revealed that expression of human pro-HB-EGF in the TG hearts was significantly decreased on the next day of DT injection, and almost disappeared on the following day (Fig. 1*E*). After 7 days, transgene-expressing cardiomyocytes were undetected in the TG hearts, suggesting that they were completely ablated through DT-mediated cytotoxicity.

DT-mediated Myocardial Cell Loss Caused Heart Failure in Mice—We next examined the geometric, functional, and histological changes in the hearts caused by DT-mediated myocardial cell damages. Gross inspections of the TG hearts 7 days after DT injection showed global chamber dilatation with marked wall thinning and atrial thrombus (Fig. 2*A*), and the heart to body weight ratios were ~1.3-fold increased (Fig. 2*B*), whereas the mock-treated TG hearts and DT- or mock-treated WT hearts showed no geometric change (Fig. 2).

To evaluate cardiac function, we performed transthoracic echocardiographic examination. Seven days after injection, a ~1.3-fold increase in the left ventricular end-diastolic dimension and a 1.5–1.7-fold decrease in left ventricular wall thickness were observed in DT-treated TG, whereas these parameters were unchanged in mock-treated TG (Fig. 2, *C* and *D*) and DT- or mock-treated WT. Echocardiographic examination also demonstrated a 2.4-fold reduction in % FS in DT-treated TG. These results suggest that injection of DT induced deterioration of LV systolic function with chamber dilatation and ventricular wall thinning in TG. In contrast, no discernible phenotype was observed in TG in the absence of DT, and DT had no harmful effect on WT.

Hematoxylin-eosin staining of the histological sections of TG hearts 7 days after DT injection revealed degenerated cardiomyocytes surrounded by inflammatory cells (Fig. 3*A*). These pathological findings were not observed in WT with or without DT injection (data not shown). The infiltrating inflammatory cells were identified as macrophages by immunohistochemical analysis using anti-Mac-3 antibody (Fig. 3*B*). Histological sections with Masson's trichrome staining showed interstitial fibrosis in DT-treated TG hearts (Fig. 3*A*). Silver staining of the

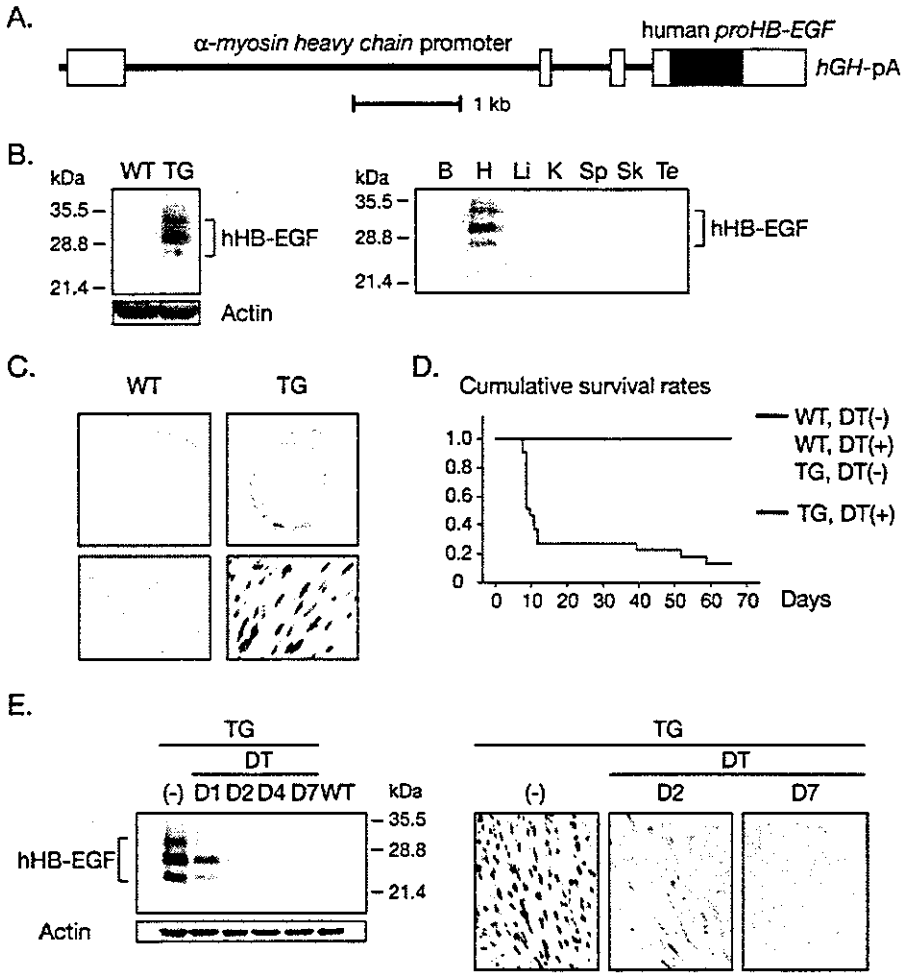

FIG. 1. **DT-induced myocardial cell ablation in transgenic mice expressing human *pro-HB-EGF*.** *A*, schematic representation of the transgene containing α-myosin heavy chain (*αMHC*) promoter, human *pro-HB-EGF* cDNA, and human growth hormone (*GH*) polyadenylation signal (*pA*). *B*, Western blot analysis using an antibody specific for human pro-HB-EGF revealed transgene expression in TG hearts (*left*). Expression of human pro-HB-EGF in TG was observed specifically in the hearts (*right*). *B*, brain; *H*, heart; *Li*, liver; *K*, kidney; *Sp*, spleen; *Sk*, skeletal muscle; *Te*, testis. *C*, *in situ* hybridization analysis using a riboprobe specific for human *pro-HB-EGF*. Transgene was expressed in a mosaic pattern, and cardiomyocytes expressing the transgene were 17.3 ± 6.0% of the total cardiomyocytes within TG hearts. *D*, Kaplan-Meier survival curves of control mice (WT treated with mock or DT and TG treated with mock, $n = 21$, respectively) and TG ($n = 21$) treated with intramuscular injection of DT. *E*, complete ablation of transgene-expressing cardiomyocytes following DT injection revealed by immunoblot (*left*) and *in situ* hybridization analysis. Expression of pro-HB-EGF was remarkably diminished on day 2 (*D2*) and was completely undetected on day 7 (*D7*).

sections of TG hearts on 14 days after DT injection revealed a 1.9-fold increase in cross-sectional areas of cardiomyocytes (Fig. 3*C*), indicating that the cardiomyocytes, which did not express the transgene and survived DT administration, underwent hypertrophic cell growth.

Alterations of Gene Expression in TG Presenting DT-induced Heart Failure—To characterize the molecular basis of heart failure caused by DT-induced myocardial cell ablation, we examined expression levels of several molecular markers. Expression of *BNP* was up-regulated 1 day after DT injection, and persistently elevated thereafter (Fig. 4). Increased expression of skeletal α-actin and decreased expression of *SERCA2* were evident 4 days after DT injection (Fig. 4). Up-regulation of natriuretic peptide genes and fetal cardiac genes including skeletal α-actin is one of the characteristic cellular responses observed during cardiac hypertrophy (32, 33). Especially, ventricular expression of *BNP* is induced promptly in response to volume expansion and pressure overload, and plasma BNP concentrations have proven to be valuable for diagnostic and prognostic assessment in patients with heart failure (34). In addition, down-regulation of *SERCA2* has been reported to be a sensitive marker for heart failure (35). Therefore, these patterns of cardiac gene expression indicated that DT-induced myocardial cell ablation burdened hemodynamic overload and progressed overt heart failure concomitantly with cardiac hypertrophy.

Consistent with the histological finding of infiltration by macrophages, an increase in expression of *MCP-1* was observed 1 day after DT injection, and expression levels of *MCP-1* were further increased until 4 days and declined on 7 days (Fig. 4). The expression levels of *TNF-α*, encoding an inflammatory cytokine produced by macrophages, changed in parallel with that of *MCP-1* (Fig. 4). Insomuch as symptomatic heart failure was evident 7 days after DT injection, stressed myocardium could be another source of *TNF-α* production at this period. Following up-regulation of inflammatory markers, expression levels of the collagen genes (*Col1a2* and *Col3a1*) were increased at 4 days after DT injection (Fig. 4). These temporal profiles of

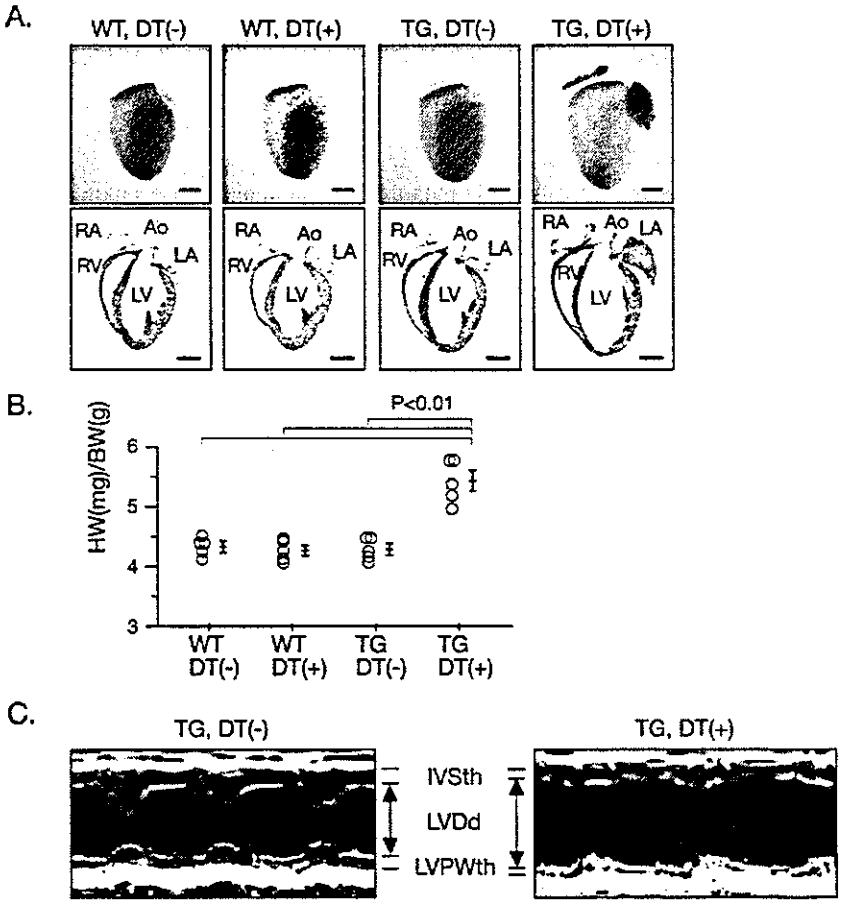

D.

	WT, DT(-)	WT, DT(+)	TG, DT(-)	TG, DT(+)
Number	10	10	10	10
Age (weeks)	10.7±0.4	10.6±0.5	11.5±0.3	10.9±0.3
BW(g)	24.0±1.7	24.1±1.2	24.8±0.4	24.3±1.3
HR (beats/min.)	261.0±15.9	258.9±18.8	256.3±18.4	252.3±18.0
LVDd (mm)	3.69±0.14	3.71±0.17	3.75±0.23	4.69±0.71
LVDs (mm)	2.05±0.13	2.11±0.20	2.08±0.27	3.81±0.46
FS (%)	44.2±4.7	43.2±4.9	47.4±3.5	19.4±3.0
IVSth (mm)	0.65±0.03	0.65±0.03	0.66±0.02	0.45±0.03
LVPWth (mm)	0.65±0.03	0.66±0.02	0.66±0.02	0.39±0.03

FIG. 2. **DT-induced cardiomyocyte loss caused heart failure in mice.** *A*, gross morphology of whole hearts (*upper rows*) and longitudinal sections (*lower rows*) of WT and TG 7 days after DT or mock injection. *Ao*, aorta; *LA*, left atrium; *LV*, left ventricle; *RA*, right atrium; *RV*, right ventricle. *Bar*, 2 mm. *B*, increase in heart to body weight ratios observed in TG 7 days after DT injection. *C*, representative M-mode echocardiograms. *IVS*, interventricular septum; *LVPW*, left ventricular posterior wall. *D*, echocardiographic measurements. *BW*, body weight; *FS*, fractional shortening; *HR*, heart rate; *IVSth*, interventricular thickness in end-diastole; *LVDd*, left ventricular diameter in end-diastole; *LVDs*, left ventricular diameter in end-systole; *LVPWth*, left ventricular posterior wall thickness in end-diastole.

gene expressions suggest that mobilization of macrophages are induced by up-regulated MCP-1 after the myocardial cell ablation, leading to cardiac fibrosis by enhanced production of inflammatory cytokines, and that inflammatory cytokines and cardiac remodeling might promote left ventricular dysfunction evoked by myocardial cell loss.

Myocardial Cell Death Induced by DT Is Not Primarily because of Apoptosis—To investigate the mechanisms of myocardial cell death in DT-treated TG hearts, we first performed a TUNEL assay. In the hearts of DT-treated TG, we could not detect any TUNEL-positive cardiomyocytes or inflammatory cells, whereas a marked increase in TUNEL-positive cells was detected in the spleen of mice treated with intraperitoneal administration of lipopolysaccharide as positive controls (Fig. 5*A*). Likewise, analysis of genomic DNA by agarose gel provided no evidence of DNA laddering in DT-treated TG hearts (Fig. 5*B*). We further examined activation of caspase 3 (Fig. 5*C*), changes in expression of proapoptotic and antiapoptotic Bcl2 family proteins (Fig. 5*D*), and cytochrome *c* release from mitochondria (Fig. 5*E*), but biochemi-

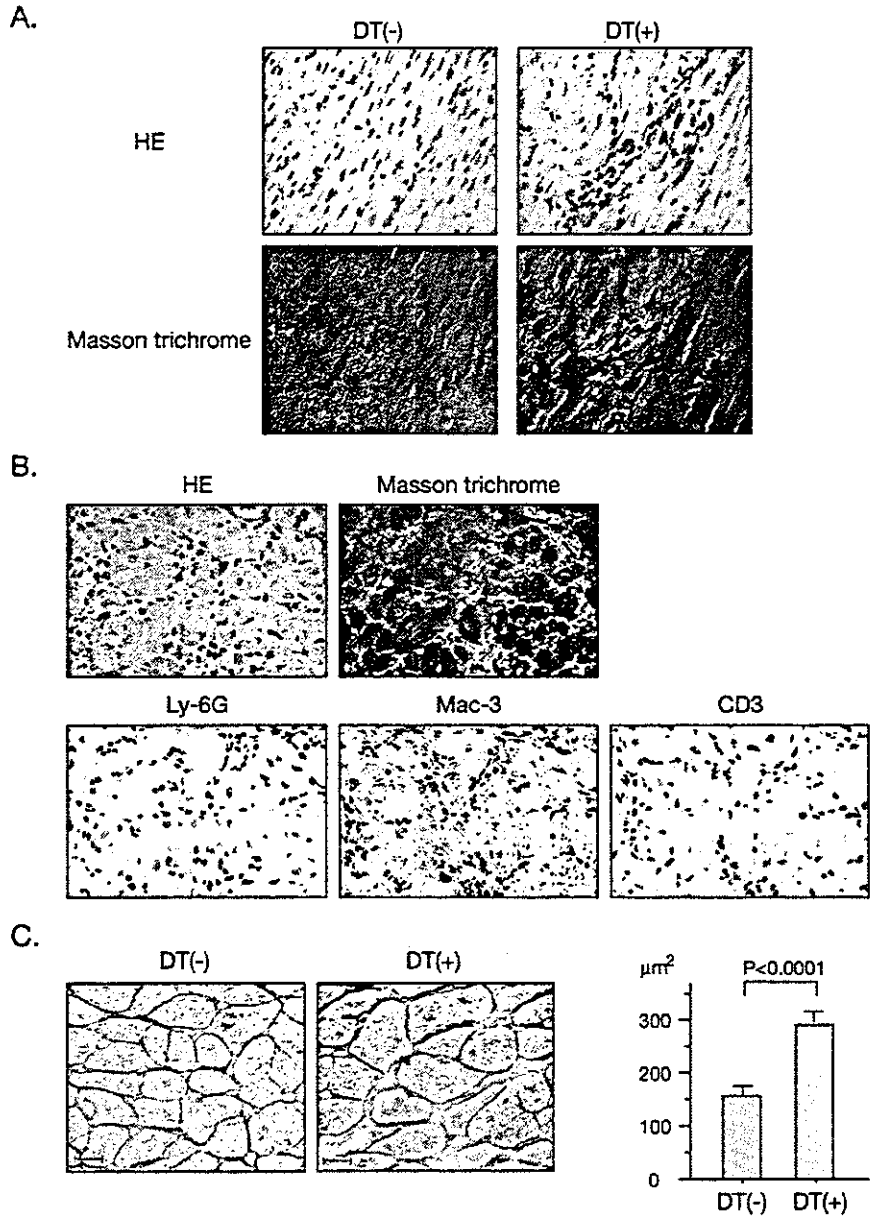

FIG. 3. **Histological analysis of the hearts after DT injection.** *A*, serial sections with hematoxylin-eosin (*HE*) staining revealed cardiomyocyte degeneration and infiltration of inflammatory cells 7 days after DT injection. Masson's trichrome staining showed interstitial fibrosis. *B*, infiltrating inflammatory cells were predominantly macrophages with positive staining for Mac-3 but not for Ly-6G nor CD3. *C*, silver staining of TG hearts 14 days after DT injection revealed an increase in the cross-sectional area of cardiomyocytes, indicating hypertrophic compensation of myocardial cells without transgene expression.

cal changes leading to typical apoptosis were not observed in DT-treated TG hearts.

Autophagy Is the Mechanism of Myocardial Cell Death in DT-induced Failing Hearts—ACD is a regulated process of caspase-independent programmed cell death, in which intracellular components are degradated by lysosomal or proteasomal proteases (21–23). Immunohistochemical analysis revealed positive staining for lysosomal protease cathepsin D, LAMP-1, and ubiquitin in cardiomyocytes of DT-treated TG hearts (Fig. 6*A*). It is notable that cathepsin D showed a diffuse cytosolic distribution, whereas LAMP-1 showed a granular localization. These results suggest an increase in formation of lysosomes and leakage of activated lysosomal enzymes into the cytosol. Recently, it has been reported that, in human failing hearts, ubiquitin accumulation in cardiomyocytes may be associated with up-regulation of ubiquitin-conjugating enzyme E2 (UBC2) and down-regulation of deubiquitinating enzymes such as UFD1 and isopeptidase T (6). However, Western blot analysis revealed that the amounts of the ubiquitin-activating enzyme E1, UBC2, ubiquitin-ligating enzyme E3 (E6-AP), and UFD1 were not unchanged in DT-treated TG hearts when compared with control hearts (Fig. 6*B*).

Electron microscopic analysis revealed abundant cytosolic vacuoles and segmented configuration of nuclei with lumpy con-

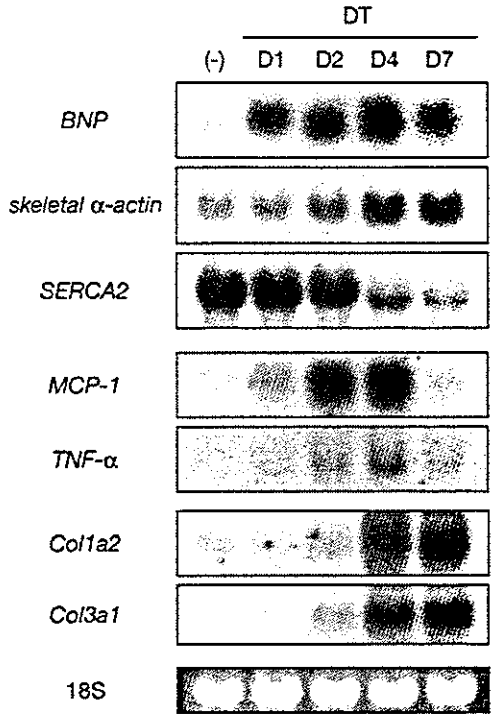

FIG. 4. **Alterations in gene expression after DT injection.** Temporal profiling of gene expression following administration of DT (5 mg/kg). Expression levels of cardiac genes, inflammatory cytokine genes, and collagen genes were examined by Northern blot analysis.

densation of chromatin in degenerated cardiomyocytes in TG hearts 3 days after DT injection (Fig. 7, *A* and *B*). However, nuclear fragmentation and crescent-shaped chromatin condensation at the nuclear periphery typical of apoptosis were not observed. In higher magnifications, cytosolic vacuoles containing lipid droplets with myelin figures and degenerated mitochondria (Fig. 7, *C* and *D*), suggested that these vacuoles are typical autophagosomes. In terminally degenerated cardiomyocytes, lysis of myofibrills and other intracellular organelles were prominent (Fig. 7*E*). These findings suggest that myocardial cell loss in DT-treated TG hearts is primarily because of ACD.

Autophagic degeneration has been implicated in human failing heart failure (3–7). We also found cardiomyocytes undergoing autophagic cell death in a biopsied specimen from a 43-year-old patient suffering from dilated cardiomyopathy. Similar to the electron micrographic findings in degenerated cardiomyocytes in our mouse model of heart failure, myofibrillar degeneration in association with cytosolic vacuoles and lipid droplets were observed in this biopsied specimen (Fig. 7*F*). The vacuoles were autophagosomes containing digested organelles. These findings are illustrative of the previously reported features characteristic of ACD in human heart failure. Therefore, degenerated cardiomyocytes in human dilated cardiomyopathy patients showed ultrastructural alterations similar to those in our mouse model of heart failure.

DISCUSSION

In this study, we generated a novel mouse model of heart failure, where cardiomyocyte loss through ACD is arbitrarily and specifically induced by intramuscular injection of DT. Recent technical progress in genetic manipulation and physiological measurements enabled us to produce several mouse models of heart failure (36). These models have improved our understanding of pathophysiology of heart failure and have been of great help for establishment and evaluation of new therapeutic approaches. Genetically engineered mice, in particular, expanded the list of gene products that are involved in generation or progression of heart failure, but they have specific limitations as animal models. For example, mice homozygous for muscle LIM protein (*MLP*) develop cardiomyopathy and heart failure, but the clinical courses of individual mice are divergent because the penetrance of phenotype is influenced by genetic backgrounds (37). About half of the *MLP*-deficient mice suffer from severe congestive heart failure and die during the second postnatal week, but the rest of the *MLP*-deficient mice survive to adulthood and are viable. Development of cardiomyopathy is also identified in tropomodulin-overexpressing transgenic mice (38). In this model, severe signs of heart failure are observed between 2 and 4 weeks after birth and most symptomatic mice die within a few days. The phenotypes of these model mice are primarily genotype-dependent, but are susceptible to the effects of genetic backgrounds. In addition, a difficulty in morphological and biochemical approach in studying a role of cardiomyocyte death in heart failure arises from the low occurrence of cell death in these models (2). In our mouse model of heart failure, cardiomyocytes expressing the DT receptor are selectively and simultaneously damaged by administration of DT, and this advantageous feature not only makes it possible to induce symptomatic heart failure arbitrarily but also provides insights into the roles of cell death in heart failure.

Our model appears conceptually similar to the one reported in the earlier work (39), in which DT-A expression is regulated by a tetracycline-responsive promoter. In that model, induction of DT-A in the hearts resulted in congestive heart failure as well. However, a leaky induction is occasionally observed in this tetracycline-inducible system, and subtle expression of DT-A might have nonspecific and undesirable effects, insomuch as the toxicity of DT-A is extremely high (17). In our model, the DT receptor, not injurious in the absence of DT, was expressed in the hearts, and myocardial cell ablation was specifically and ideally achieved.

Temporal histological analysis and profiling of gene expression revealed a series of cellular events that finally evoked heart failure (Figs. 3 and 4). Transgene expression was dramatically reduced in a few days after DT injection (Fig. 1*E*), suggesting that cardiomyocyte death occurs during that period. Following cardiomyocyte death, inflammatory cells infiltrated and produced inflammatory cytokines. Around 7 days, hemodynamic deterioration with apparent cardiac remodeling induced symptomatic heart failure. These findings strongly suggest that myocardial cell death causes symptomatic heart failure. In addition, our model allowed quantitative analysis of cardiomyocyte death. *In situ* hybridization analysis revealed that expression of the transgene was scattered diffusely and observed in 17.3 ± 6.0% of cardiomyocytes in TG hearts. Because there was no cardiomyocyte expressing the transgene on day 7 after DT injection, all of the transgene-expressing cells (~17% of cardiomyocytes) might be dead. These results suggest that loss of this population is sufficient to produce symptomatic heart failure, and this estimation is consistent with the notion that a diffuse loss of 10–20% of cardiomyocytes accounts for cardiac failure, whereas equivalent cardiac failure is produced by a segmental loss of 40–50% of cardiomyocytes after coronary artery occlusion (40).

Electron microscopic analysis revealed that, in our mouse model, damaged cardiomyocytes showed abundant cytoplasmic autophagosomes and chromatin condensation with more complex and lumpier shapes than in apoptosis, both of which are characteristic of ACD (Fig. 7). ACD is defined as a regulated pathway of cytoplasmic degradation executed by lysosomal and

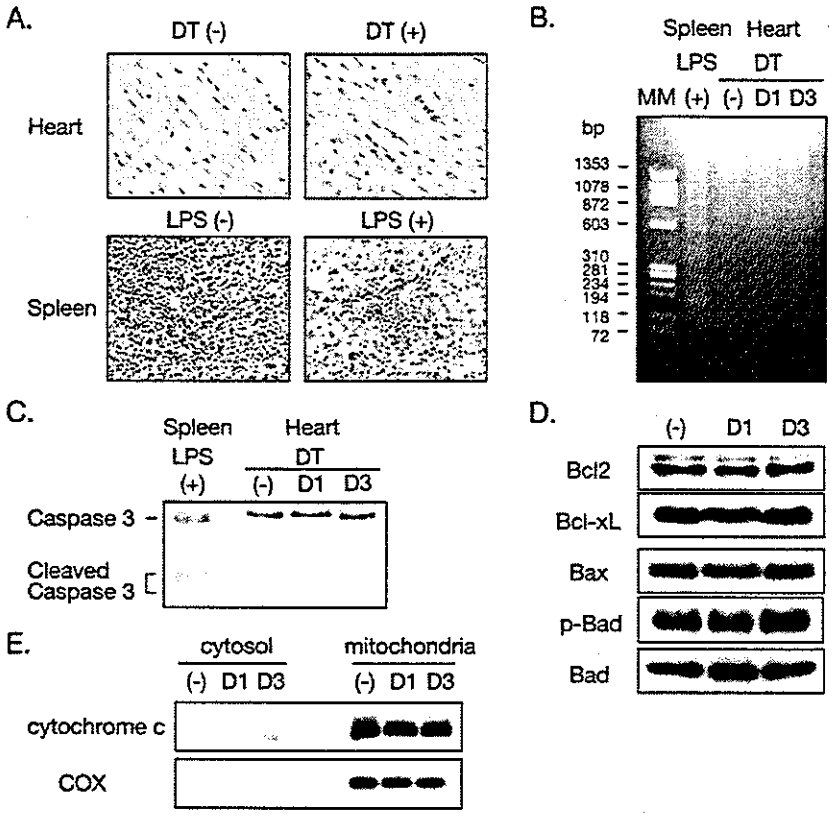

FIG. 5. **DT-induced myocardial cell death is not mediated by apoptosis, but by autophagy.** *A* and *B*, TUNEL method (*A*) and electrophoresis of genomic DNA by agarose gel (*B*) showed no evidence of DNA fragmentation in TG hearts 3 days after DT injection. Spleens from mice with lipopolysaccharide-induced sepsis were used as a positive control. *C–E*, immunoblot analysis showing no evidence of activation of caspase 3 (*C*), changes in expressions of Bcl2 family proteins (*D*) and cytochrome *c* release from mitochondria (*E*) in DT-treated TG hearts. *COX*, cytochrome c oxidase subunit IV. *D*, day. *LPS*, lipopolysaccharide.

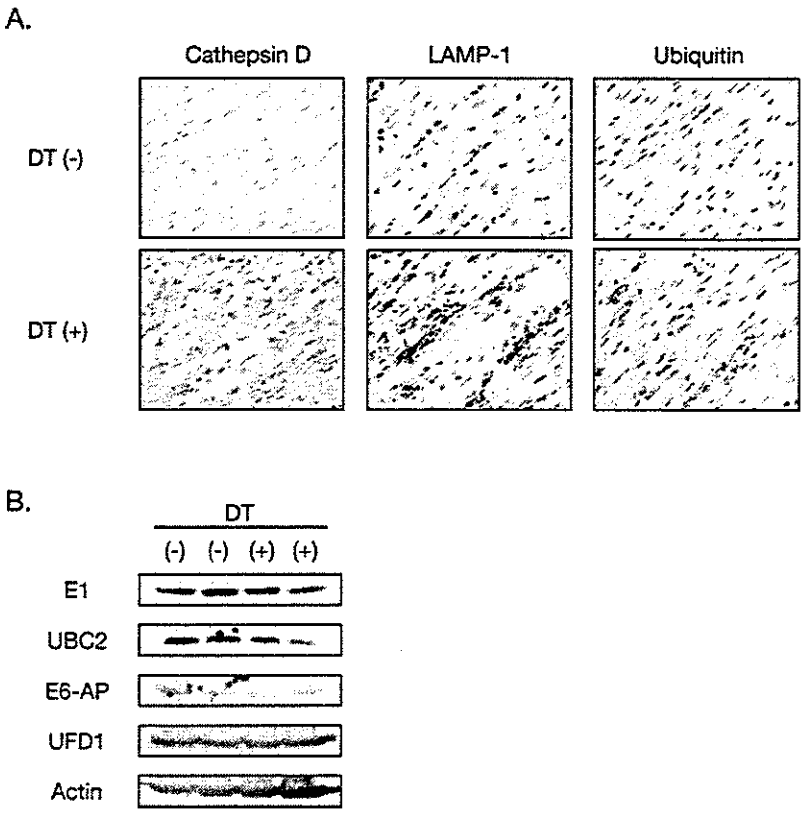

FIG. 6. **DT-induced myocardial cell death is mediated by autophagy.** *A*, immunohistochemistry showing cardiomyocytes were positively stained for cathepsin D, LAMP-1, and ubiquitin in TG hearts 3 days after DT injection. *B*, immunoblot analysis showing unchanged expression levels of the ubiquitin-activating enzyme E1, ubiquitin-conjugating enzyme E2 (*UBC2*), ubiquitin-ligating enzyme E3 (*E6-AP*), and deubiquitinating enzyme UFD1.

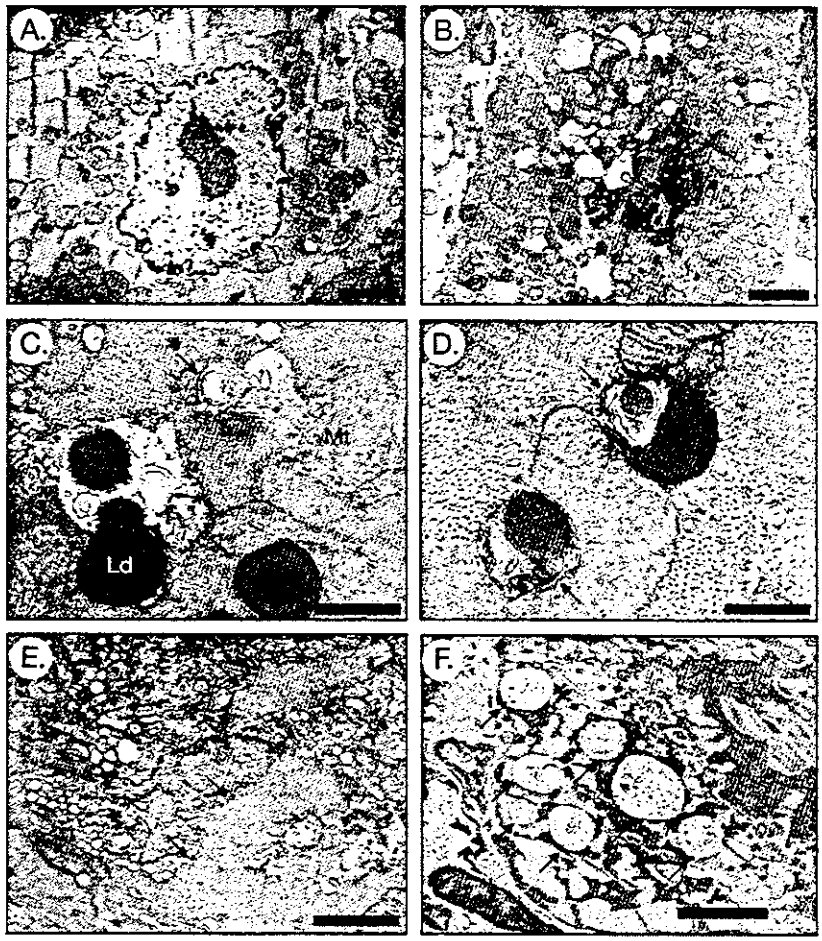

FIG. 7. **Electron microscopic analysis of the hearts after DT injection.** Electron microscopic analysis before (*A*) and after DT injection (*B–E*). In cardiomyocytes of DT-treated TG hearts, nuclear morphological changes associated with lumpy chromatin condensation were observed (*arrow* in *B*). Abundant vacuoles of various sizes in the cytoplasm (*B*) were typical autophagosomes containing degenerating lipid droplets and mitochondria (*C* and *D*). *Arrows* (in *C* and *D*) indicate myelin figures. Myofibrillar lysis (*arrows*) was observed in cardiomyocytes undergoing autophagic cell death (*E*). Electron microscopic analysis of biopsied myocardium from a patient with dilated cardiomyopathy (*F*) revealed cardiomyocytes containing many autophagosomes with degenerating mitochondria (*arrows*). *Ld*, lipid droplet; *Mt*, mitochondria. *Bars*, 2 μm (*A* and *B*), 1 μm (*C* and *E*), 0.5 μm (*D*), and 5 μm (*F*).

proteasomal proteases (21–23, 41). Consistently, elevated expressions of cathepsin D and ubiquitin were recognized in DT-treated TG cardiomyocytes (Fig. 6*A*). In contrast, biochemical signals inducing apoptosis were not activated. ACD often occurs in large, cytoplasmic-rich, and post-mitotic cells, and has been implicated in several human diseases (19, 21–23, 41). For example, ACD is associated with neurodegenerative diseases such as Parkinson's disease (42), Huntington's disease (43), and Alzheimer's disease (44). Degenerated cardiomyocytes displaying morphological features characteristic of ACD have recently been reported to exist in the failing hearts of patients with dilated cardiomyopathy, valvular heart diseases, congenital heart diseases, and hypertensive heart diseases (Fig. 7*F*) (3–7). A recent paper demonstrated that cardiomyocyte apoptosis of rare occurrence comparable with that observed in human failing hearts were sufficient to cause lethal cardiomyopathy in transgenic mice with a ligand-induced caspase-8 activation in the hearts (45). It is noteworthy that autophagic cardiomyocyte death has been reported to be detectable more frequently than apoptosis or oncosis in failing or hemodynamically overloaded human hearts (3, 6, 7), although the frequency of the each form of cell death may be influenced by disease stages and backgrounds (*e.g.* age, etiology, clinical feature, and treatment) of the examined samples (2).

Recent studies have indicated a significant role of lysosomal cysteine and aspartic protease cathepsins in execution of ACD (21, 46). PC12 cells cultured in a serum-deprived condition showed morphological features characteristic of ACD with an increase in proteolytic activity of cathepsin D (46), and forced expression of cathepsin D in PC12-induced rapid cell death, indicating a regulatory role of cathepsin D in ACD. Expression of cathepsin D was increased in DT-treated TG hearts (Fig. 6*A*). In damaged cardiomyocytes, translocation of cathepsin D from lysosomes to the cytosol was evident, which is indicative of enhanced proteolytic activity (47). Cathepsin D has been reported to be activated in human failing hearts (5) and also to be a positive mediator of apoptotic cell death (22, 47). Further experiments are required to clarify whether cathepsin D is involved in execution of myocardial ACD in the pathogenesis of heart failure and how cathepsin D regulates these modes of cell death differentially.

According to the recent studies, ubiquitin-dependent protein degradation is linked to autophagy (48). Accumulation of ubiquitin in cardiomyocytes was observed in DT-treated TG hearts (Fig. 6*A*) as well as in human failing hearts (4, 6, 7). Kostin *et al.* (6) demonstrated a functional defect in the ubiquitin/proteasome pathway together with ubiquitin accumulation in human failing hearts, and speculated that an excess of ubiquitinated proteins might activate autophagic protein degradation. The precise molecular mechanisms of how ubiquitin accumulation enhances autophagy remain unknown, although ubiquitination is postulated to be required for maturation of autophagosomes (48). Unlike human failing hearts (6), the amounts of UBC2 and UFD1 were unchanged in the hearts of our model mice (Fig. 6B). Protein ubiquitination and deubiquitination are mediated by a large number of enzymes (49), and it is an important issue to be

addressed in the future how ubiquitin is accumulated in cardiomyocytes undergoing autophagic cell death.

Diphtheria is a communicable disease affecting the upper respiratory tract and occasionally the skin as primary infection (50). However, remote organs such as heart or peripheral nerves are often damaged when DT is absorbed into the systemic circulation. Although diphtheria infection has been rarely encountered in developed countries because of the high rates of vaccination after the mid 1960s, several sporadic outbreaks occurred, for example, in the former Union of Soviet Socialist Republics in 1990s (50). Myocardial involvement is a major complication that determines the prognosis, but the pathophysiology associated with diphtheritic cardiomyopathy remains largely unknown. Histological analysis of the postmortal heart of a diphtheria patient revealed hyaline degeneration of myocardium and infiltration of mononuclear cells, and cytosolic lipid droplets and clumped chromatin granules were observed by electron microscopic examination (51). Although vacuoles of autophagosomes were not described in this paper, these findings were similar to those observed in our mouse model. Interestingly, cardiomyocyte loss through ACD associated with a decrease in protein synthesis was also observed in anthracycline-induced cardiomyopathy (52). Therefore, autophagic cardiomyocyte death evoked by a decrease in protein synthesis might not be confined to diphtheritic cardiomyopathy, but a more generalized phenomenon that occurs during progression of heart failure arising from miscellaneous etiologies. In this regard, our model of experimentally induced heart failure will be useful to elucidate molecular mechanisms underlying structural and functional changes associated with ACD in heart failure.

Acknowledgments—We thank R. Kobayashi, E. Fujita, and M. Iida for excellent technical assistance. We are grateful to Dr. A. Ullrich (Max-Planck-Institute of Biochemistry, Martinsried, Germany) and Dr. J. Robbins (Children's Hospital, Cincinnati, OH) for providing cDNAs.

REFERENCES

1. Nadal, G. B., Kajstura, J., Leri, A., and Anversa, P. (2003) *Circ. Res.* **92,** 139–150
2. Kang, P. M., and Izumo, S. (2000) *Circ. Res.* **86,** 1107–1113
3. Yamamoto, S., Sawada, K., Shimomura, H., Kawamura, K., and James, T. N. (2000) *J. Mol. Cell Cardiol.* **32,** 161–175
4. Knaapen, M. W., Davies, M. J., De, B. M., Haven, A. J., Martinet, W., and Kockx, M. M. (2001) *Cardiovasc. Res.* **51,** 304–312
5. Shimomura, H., Terasaki, F., Hayashi, T., Kitaura, Y., Isomura, T., and Suma, H. (2001) *Jpn. Circ. J.* **65,** 965–968
6. Kostin, S., Pool, L., Elsasser, A., Hein, S., Drexler, H. C., Arnon, E., Hayakawa, Y., Zimmermann, R., Bauer, E., Klovekorn, W. P., and Schaper, J. (2003) *Circ. Res.* **92,** 715–724
7. Hein, S., Arnon, E., Kostin, S., Schonburg, M., Elsasser, A., Polyakova, V., Bauer, E. P., Klovekorn, W. P., and Schaper, J. (2003) *Circulation* **107,** 984–991
8. Mann, D. L. (1999) *Circulation* **100,** 999–1008
9. Schaper, J., Elsasser, A., and Kostin, S. (1999) *Circ. Res.* **85,** 867–869
10. Anversa, P. (2000) *Circ. Res.* **86,** 121–124
11. Pappenheimer, A. J. (1977) *Annu. Rev. Biochem.* **46,** 69–94
12. Falnes, P. O., and Sandvig, K. (2000) *Curr. Opin. Cell Biol.* **12,** 407–413
13. Van Ness, B. G., Howard, J. B., and Bodley, J. W. (1980) *J. Biol. Chem.* **255,** 10710–10716
14. Higashiyama, S., Abraham, J. A., Miller, J., Fiddes, J. C., and Klagsbrun, M. (1991) *Science* **251,** 936–939
15. Naglich, J. G., Metherall, J. E., Russell, D. W., and Eidels, L. (1992) *Cell* **69,** 1051–1061
16. Mitamura, T., Umata, T., Nakano, F., Shishido, Y., Toyoda, T., Itai, A., Kimura, H., and Mekada, E. (1997) *J. Biol. Chem.* **272,** 27084–27090
17. Saito, M., Iwawaki, T., Taya, C., Yonekawa, H., Noda, M., Inui, Y., Mekada, E., Kimata, Y., Tsuru, A., and Kohno, K. (2001) *Nat. Biotechnol.* **19,** 746–750
18. Kim, J., and Klionsky, D. J. (2000) *Annu. Rev. Biochem.* **69,** 303–342
19. Klionsky, D. J., and Emr, S. D. (2000) *Science* **290,** 1717–1721
20. Ohsumi, Y. (2001) *Nat. Rev. Mol. Cell. Biol.* **2,** 211–216
21. Bursch, W. (2001) *Cell Death Differ.* **8,** 569–581
22. Leist, M., and Jaattela, M. (2001) *Nat. Rev. Mol. Cell. Biol.* **2,** 589–598
23. Lockshin, R. A., and Zakeri, Z. (2002) *Curr. Opin. Cell Biol.* **14,** 727–733
24. Takano, H., Nagai, T., Asakawa, M., Toyozaki, T., Oka, T., Komuro, I., Saito, T., and Masuda, Y. (2000) *Circ. Res.* **87,** 596–602
25. Asakawa, M., Takano, H., Nagai, T., Uozumi, H., Hasegawa, H., Kubota, N., Saito, T., Masuda, Y., Kadowaki, T., and Komuro, I. (2002) *Circulation* **105,** 1240–1246
26. Toko, H., Zhu, W., Takimoto, E., Shiojima, I., Hiroi, Y., Zou, Y., Oka, T., Akazawa, H., Mizukami, M., Sakamoto, M., Terasaki, F., Kitaura, Y., Takano, H., Nagai, T., Nagai, R., and Komuro, I. (2002) *J. Biol. Chem.* **277,** 24735–24743
27. Akazawa, H., Komuro, I., Sugitani, Y., Yazaki, Y., Nagai, R., and Noda, T. (2000) *Genes Cells* **5,** 499–513
28. Vander, H. M., Chandel, N. S., Williamson, E. K., Schumacker, P. T., and Thompson, C. B. (1997) *Cell* **91,** 627–637
29. Saito, S., Hiroi, Y., Zou, Y., Aikawa, R., Toko, H., Shibasaki, F., Yazaki, Y., Nagai, R., and Komuro, I. (2000) *J. Biol. Chem.* **275,** 34528–34533
30. Chau, B. N., Borges, H. L., Chen, T. T., Masselli, A., Hunton, I. C., and Wang, J. Y. (2002) *Nat. Cell Biol.* **4,** 757–765
31. Komazaki, S., Ito, K., Takeshima, H., and Nakamura, H. (2002) *FEBS Lett.* **524,** 225–229
32. Komuro, I., and Yazaki, Y. (1993) *Annu. Rev. Physiol.* **55,** 55–75
33. Sadoshima, J., and Izumo, S. (1997) *Annu. Rev. Physiol.* **59,** 551–571
34. de Lemos, J. A., McGuire, D. K., and Drazner, M. H. (2003) *Lancet* **362,** 316–322
35. Mercadier, J. J., Lompre, A. M., Duc, P., Boheler, K. R., Fraysse, J. B., Wisnewsky, C., Allen, P. D., Komajda, M., and Schwartz, K. (1990) *J. Clin. Investig.* **85,** 305–309
36. Elsner, D., and Riegger, G. A. (1995) *Curr. Opin. Cardiol.* **10,** 253–259
37. Arber, S., Hunter, J. J., Ross, J. J., Hongo, M., Sansig, G., Borg, J., Perriard, J. C., Chien, K. R., and Caroni, P. (1997) *Cell* **88,** 393–403
38. Sussman, M. A., Welch, S., Cambon, N., Klevitsky, R., Hewett, T. E., Price, R., Witt, S. A., and Kimball, T. R. (1998) *J. Clin. Investig.* **101,** 51–61
39. Lee, P., Morley, G., Huang, Q., Fischer, A., Seiler, S., Horner, J. W., Factor, S., Vaidya, D., Jalife, J., and Fishman, G. I. (1998) *Proc. Natl. Acad. Sci. U. S. A.* **95,** 11371–11376
40. Anversa, P., Zhang, X., Li, P., and Capasso, J. (1992) *J. Clin. Investig.* **89,** 618–629
41. Lockshin, R. A., Osborne, B., and Zakeri, Z. (2000) *Cell Death Differ.* **7,** 2–7
42. Anglade, P., Vyas, S., Javoy-Agid, F., Herrero, M. T., Michel, P. P., Marquez, J., Mouatt-Prigent, A., Ruberg, M., Hirsch, E. C., and Agid, Y. (1997) *Histol. Histopathol.* **12,** 25–31
43. Kegel, K. B., Kim, M., Sapp, E., McIntyre, C., Castano, J. G., Aronin, N., and DiFiglia, M. (2000) *J. Neurosci.* **20,** 7268–7278
44. Cataldo, A. M., Hamilton, D. J., Barnett, J. L., Paskevich, P. A., and Nixon, R. A. (1996) *J. Neurosci.* **16,** 186–199
45. Wencker, D., Chandra, M., Nguyen, K., Miao, W., Garantziotis, S., Factor, S. M., Shirani, J., Armstrong, R. C., and Kitsis, R. N. (2003) *J. Clin. Investig.* **111,** 1497–1504
46. Uchiyama, Y. (2001) *Arch. Histol. Cytol.* **64,** 233–246
47. Roberg, K., and Ollinger, K. (1998) *Am. J. Pathol.* **152,** 1151–1156
48. Blommaart, E. F., Luiken, J. J., and Meijer, A. J. (1997) *Histochem. J.* **29,** 365–385
49. Pickart, C. M. (2004) *Cell* **116,** 181–190
50. Hadfield, T. L., McEvoy, P., Polotsky, Y., Tzinserling, V. A., and Yakovlev, A. A. (2000) *J. Infect. Dis.* **181,** Suppl. 1, S116–S120
51. Burch, G. E., Sun, S. C., Sohal, R. S., Chu, K. C., and Colcolough, H. L. (1968) *Am. J. Cardiol.* **21,** 261–268
52. Semenov, D. E., Lushnikova, E. L., and Nepomnyashchikh, L. M. (2001) *Bull. Exp. Biol. Med.* **131,** 505–510

THE JOURNAL OF BIOLOGICAL CHEMISTRY
Vol. 279, No. 12, Issue of March 19, pp. 11384–11391, 2004
Printed in U.S.A.

Adult Cardiac Sca-1-positive Cells Differentiate into Beating Cardiomyocytes*[S]

Received for publication, October 1, 2003, and in revised form, December 16, 2003
Published, JBC Papers in Press, December 31, 2003, DOI 10.1074/jbc.M310822200

Katsuhisa Matsuura‡§, Toshio Nagai‡, Nobuhiro Nishigaki‡¶, Tomomi Oyama‡, Junichiro Nishi‡, Hiroshi Wada‡, Masanori Sano‡, Haruhiro Toko‡, Hiroshi Akazawa‡, Toshiaki Sato‖, Haruaki Nakaya‖, Hiroshi Kasanuki§, and Issei Komuro‡**

From the ‡Department of Cardiovascular Science and Medicine, Chiba University Graduate School of Medicine, Chiba 260-8670, Japan, the §Department of Cardiology, The Heart Institute of Japan, Tokyo Women's Medical University, Tokyo 162-0054, Japan, the ¶Takeda Chemical Industries, LTD, Osaka 540-8645, Japan, and the ‖Department of Pharmacology, Chiba University Graduate School of Medicine, Chiba 260-8670, Japan

Although somatic stem cells have been reported to exist in various adult organs, there have been few reports concerning stem cells in the heart. We here demonstrate that Sca-1-positive (Sca-1+) cells in adult hearts have some of the features of stem cells. Sca-1+ cells were isolated from adult murine hearts by a magnetic cell sorting system and cultured on gelatin-coated dishes. A fraction of Sca-1+ cells stuck to the culture dish and proliferated slowly. When treated with oxytocin, Sca-1+ cells expressed genes of cardiac transcription factors and contractile proteins and showed sarcomeric structure and spontaneous beating. Isoproterenol treatment increased the beating rate, which was accompanied by the intracellular Ca^{2+} transients. The cardiac Sca-1+ cells expressed oxytocin receptor mRNA, and the expression was up-regulated after oxytocin treatment. Some of the Sca-1+ cells expressed alkaline phosphatase after osteogenic induction and were stained with Oil-Red O after adipogenic induction. These results suggest that Sca-1+ cells in the adult murine heart have potential as stem cells and may contribute to the regeneration of injured hearts.

The heart has long been thought to adapt to increased work and loss of cardiomyocytes by the cellular hypertrophy of residual cardiomyocytes, but not by the proliferation of mature cardiomyocytes or the differentiation of undifferentiated cells. However, recent reports have suggested that adult cardiomyocytes can proliferate under certain pathologic conditions and that there are cells expressing stem cell markers in the adult heart (1–4). It has been reported that Sca-1- and c-kit-positive (+) cells exist in the adult heart (5) and that adult murine hearts contain potential stem cells; side population (SP)[1] cells (6, 7). However, it remains to be clarified whether these cells have the characteristics of stem cells such as abilities of self-renewal and differentiation into various types of cells including mature cardiomyocytes.

Sca-1 is a member of the Ly-6 family and has first reported as one of the cell surface markers of hematopoietic stem cells (8). Recently many reports have demonstrated that multipotential stem cells derived from bone marrow and skeletal muscle express Sca-1. Okumoto *et al.* (9) have reported that Sca-1+ cells from bone marrow differentiate into hepatocyte when treated with hepatic growth factor. Gojo *et al.* (10) have reported that adult mesenchymal stem cells from bone marrow abundantly express Sca-1 and differentiate into cardiomyocyte *in vivo*. Qu-Petersen *et al.* (11) have shown that skeletal muscle-derived stem cells, which highly express Sca-1, contribute to the regeneration of the skeletal muscle in a mouse model of Duchenne muscle dystrophy. They also demonstrated that the skeletal muscle-derived stem cells were able to differentiate into neural cells and endothelial cells. Asakura *et al.* (12) have reported that ~90% of SP cells in skeletal muscle express Sca-1. It has been reported that skeletal muscle-derived Sca-1+ and CD34+ cells restore dystrophin in mdx mice (13) and that CD34+ and CD45− cells in the interstitial spaces of skeletal muscle, which highly express Sca-1, differentiate into adipocytes, endothelial, and myogenic cells (14). These findings suggest that Sca-1 might be important evidence for somatic stem cells.

Currently little is known about the humoral or growth factors that induce cardiomyogenic differentiation. It has been shown that ectopic application of bone morphological protein (BMP) 2 and 4 elicits cardiogenic responses in the chick *in vivo* system (15), and fibroblast growth factor (FGF) 2 and 4, combined with BMP-2 or BMP-4 can induce cardiogenesis in chick non-precardiac mesoderm (16). The non-canonical Wnt/c-Jun-N-terminal kinase pathways have been reported to be essential for cardiac induction in frog and chick embryo systems (17, 18). These factors are prerequisites for early cardiac differentiation but are not sufficient for accomplishing differentiation into mature beating cardiomyocytes. Recently Paquin *et al.* (19) have reported that oxytocin induces differentiation of P19 embryonic carcinoma cells to beating cardiomyocytes. In support of the role of oxytocin in cardiac development, the oxytocin receptor is increased at the protein level in the murine heart from day 7 of gestation, when cardiac differentiation starts

* This study was supported by a grant-in-aid for Scientific Research, Developmental Scientific Research, and Scientific Research on Priority Areas from the Ministry of Education, Science, Sports, and Culture, Takeda Medical Research Foundation, Uehara Memorial Foundation, grant-in-aid of The Japan Medical Association, The Kato Memorial Trust for Nambyo Research, Takeda Science Foundation, and a Japan Heart Foundation Research Grant. The costs of publication of this article were defrayed in part by the payment of page charges. This article must therefore be hereby marked "*advertisement*" in accordance with 18 U.S.C. Section 1734 solely to indicate this fact.

[S] The on-line version of this article (available at http://www.jbc.org) contains Supplementary Data.

** To whom correspondence should be addressed: Dept. of Cardiovascular Science and Medicine, Chiba University Graduate School of Medicine, 1-8-1 Inohana, Chuo-ku, Chiba 260-8670 Japan. Tel.: 81-43-226-2097; Fax: 81-43-226-2096; E-mail: komuro-tky@umin.ac.jp.

[1] The abbreviations used are: SP, side population; PE, phycoerythrin; PBS, phosphate-buffered saline; FBS, fetal bovine serum; MHC, myosin heavy chain; MLC, myosin light chain; MACS, Magnetic Cell Sorting; ALP, alkaline phosphatase; MEF, muscle enhancer factor.

TABLE I
PCR primers and PCR conditions

Primer	Product size	Annealing temperature
	bp	*°C*
α-MHC		
5′-GGAAGAGTGAGCGGCCATCAAGG-3′	302	65
5′-CTGCTGGAGAGGTTATTCCTCG-3′		
β-MHC		
5′-GCCAACACCAACCTGTCCAAGTTC-3′	205	66
5′-TGCAAAGGCTCCAGGTCTGAGGGC-3′		
MLC-2a		
5′-CAGACCTGAAGGAGACCT-3′	286	54
5′-GTCAGCGTAAACAGTTGC-3′		
MLC-2v		
5′-GCCAAGAAGCGGATAGAAGG-3′	499	55
5′-CTGTGGTTCAGGGCTCAGTC-3′		
Cardiac α-actin		
5′-CTGAGATGTCTCTCTCTCTCTTAG-3′	99	60
5′-ACAATGACTGATGAGAGATG-3′		
Csx/Nkx-2.5		
5′-CAGTGGAGCTGGACAAAGCC-3′	216	55
5′-TAGCGACGGTTCTGGAATTT-3′		
GATA4		
5′-CTGTCATCTCACTATGGGCA-3′	275	60
5′-CCAAGTCCGAGCAGGAATTT-3′		
MEF-2C		
5′-GGCCATGGTACACCGAGTACAACGAGC-3′	401	62
5′-GGGGATCCCTGTGTTACCTGCACTTGG-3′		
Oxytocin receptor		
5′-AAGATGACCTTCATCATTGTTC-3′	303	61
5′-CGACTCAGGACGAAGGTGGAGGA-3′		
ALP		
5′-TTGAAACTCCAAAAGCTCAACACCA-3′	450	62
5′-TCTCGTTATCCGAGTACCAGTCCC-3′		
Osteocalcin		
5′-CCGGGAGCAGTGTGAGCTTA-3′	92	62
5′-TAGATGCGTTTGTAGGCGGTC-3′		
β-Actin		
5′-GGACCTGGCTGGCCGGGACC-3′	583	60
5′-GCGGTGCACGATGGAGGGGC-3′		

(20). Although the precise mechanism of the effect of oxytocin is not clear, oxytocin may play an important role in the differentiation into cardiomyocytes from primitive cells including adult somatic stem cells. Here, we first report that a novel population from Sca-1+ cells derived from the adult murine heart proliferates and differentiates into beating cardiomyocytes with oxytocin treatment.

EXPERIMENTAL PROCEDURES

Animals and Reagents—Wild mice (C57Bl/6) were purchased from Takasugi Experimental Animals Supply, Co, LTD, Japan. All protocols were approved by the Institutional Animal Care and Use Committee of Chiba University. Phycoerythrin (PE) -conjugated anti-Sca-1 (anti-Ly6A/E), anti-c-kit (anti-CD117) antibodies were purchased from eBioscience (San Diego, CA). PE-conjugated anti-CD34, anti-CD45, and biotin-conjugated anti-Sca-1 antibodies were purchased from BD Pharmingen (San Diego, CA). The following antibodies were used for immunostaining: mouse monoclonal anti-cardiac troponin T (RV-C2, DSMZ-Deutsche Sammlung von Mikroorganismen und Zellkulturen GmbH, Germany), rabbit polyclonal anti-atrial natriuretic factor-1 (ANF) (Peninsula Laboratories, San Carlos. CA), goat polyclonal anti-GATA4 (Santa Cruz Biotechnology, Santa Cruz, CA), mouse monoclonal anti-myosin light chain-2v (MLC-2v) (BioCytex, France), mouse monoclonal anti-tropomyosin (Sigma Aldrich), mouse monoclonal anti-sarcomeric myosin heavy chain (MF-20) (American Type Culture Collection), rabbit polyclonal anti-connexin 43 (Zymed Laboratories, South San Francisco, CA). Fluorescent secondary antibodies were purchased from Jackson ImmunoResearch Laboratory (Bar Harbor, ME). Other reagents that are not specified were obtained from Sigma-Aldrich.

Isolation and Culture of Sca-1+ Cells from the Adult Murine Heart—A heart of adult C57Bl/6 mouse (10–12 weeks old) was enzymatically dissociated into a single cell suspension as described previously (21). Enrichment of Sca-1+ cells was achieved by sorting using the Magnetic Cell Sorting (MACS) system (Miltenyl Biotec, Sunnyvale, CA). Whole primary cell suspension was incubated with PE-conjugated anti-Sca-1 antibody for 10 min on ice, washed in PBS supplemented with 3% FBS, incubated with anti-PE micro beads for 15 min at 4 °C, and washed with PBS supplemented with 3% FBS. The samples were passed through a MACS column set up in a Miltenyl magnet and the Sca-1+ cells were eluted from the column by washing with PBS supplemented with 3% FBS. To increase the purity of the Sca-1+ cells, magnetic sorting was performed one more time. The Sca-1+ cells were cultured on 1% gelatin-coated dishes with Iscove's Modified Dulbecco's Medium (IMDM) supplemented with 10% FBS, 100 μg/ml of penicillin, and 250 μg/ml of streptomycin at 37 °C in humid air with 5% CO_2. Twenty-four hours after seeding, the cells were treated with 10 μM 5′-azacytizine for the initial 72 h or 100 nM oxytocin (WAKO, Japan). After treatment, the medium was changed every 3 days.

Characterization of Cardiac Muscle-derived Stem Cells for Flow Cytometric Analysis—Sca-1+ cells were isolated by the MACS system with biotin-conjugated anti-Sca-1 antibody and anti-biotin micro beads. Magnetic sorting was repeated twice, and the cells were incubated with PE-conjugated anti-CD45 antibody, PE-conjugated anti-CD34 antibody, and PE-conjugated anti-c-kit antibody, respectively for 10 min on ice and washed with PBS supplemented with 3% FBS. The percentages of CD45+, CD34+, and c-kit+ cells were analyzed by the EPICS ALTRA flow cytometer using EXPO32 software (Beckman Coulter, Miami, FL).

RNA Extraction and Reverse Transcriptase-PCR—Total RNA was extracted from the adult murine heart, liver, and Sca-1+ cells by RNA-bee reagent (TEL-TEST, Friendswood, TX). Reverse transcriptase (RT)-PCR of genes of cardiac transcription factors, including Csx/Nkx-2.5 (22), GATA4 (23), muscle enhancer factor-2C (MEF-2C) (24), and cardiac structural proteins, including α- and β-myosin heavy chain (MHC) (25), myosin light chain-2a (MLC-2a), MLC-2v (26), cardiac α-actin (27), and oxytocin receptor (19), alkaline phosphatase (28), osteocalcin (29) were performed using 0.1 μg of total RNA. β-actin (30) was used as an internal control. The primers used in this study and PCR conditions are described in Table I. The PCR products were size-fractionated by 2% agarose gel electrophoresis.

Immunocytochemistry—Cells were fixed with 4% paraformaldehyde for 15 min at room temperature. After preblocking with PBS containing 2% donkey serum, 2% bovine serum albumin and 0.2% Nonidet P-40 for

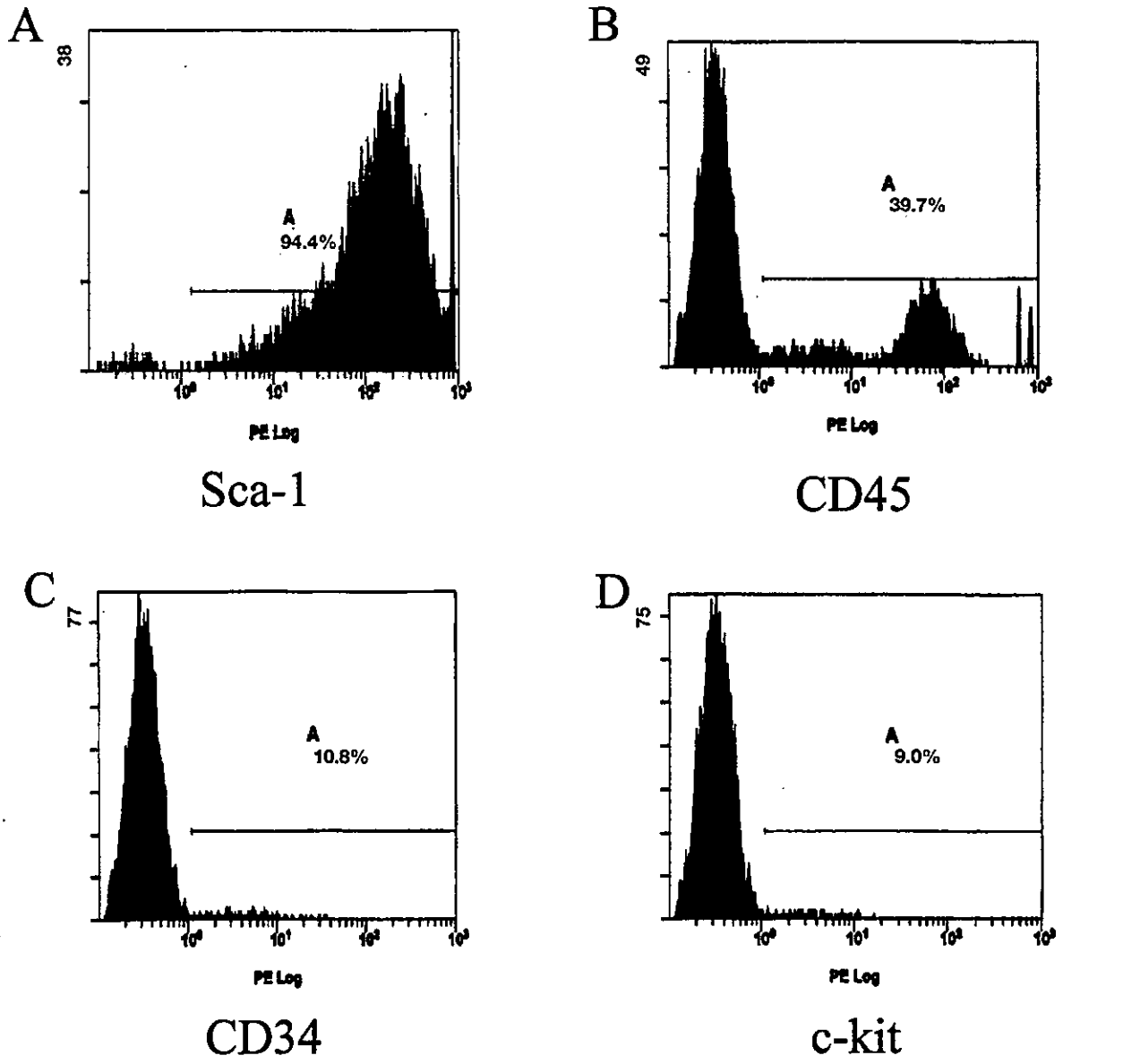

FIG. 1. **Flow cytometric analysis of Sca-1+ cells.** Sca-1+ cells were enriched by the MACS system with PE-conjugated anti-Sca-1 antibody and anti-PE micro beads, and after sorting twice, ~90% of the cells expressed Sca-1 (*A*). Sca-1+ cells were stained with PE-conjugated anti-CD45 antibody, anti-CD34 antibody, and anti-c-kit antibody. In enriched Sca-1+ cells, ~40% of the cells expressed CD45 (*B*), ~10% of the cells expressed CD34 (*C*), and c-kit (*D*).

30 min, primary antibodies in PBS containing 2% donkey serum, 2% bovine serum albumin and 0.1% Nonidet P-40 were applied overnight in 4 °C. Subsequently cells were washed three times in PBS, and then fluorescein isothiocyanate- or Cy5-conjugated secondary antibodies were applied to visualize expression of specific proteins. Nuclear staining was performed with TO-PRO-3 (Molecular Probes, Eugene, OR). Images of cells were taken by laser confocal microscopy (Radiance2000, Bio-Rad, Hercules, CA).

Phase Contrast Live Imaging—Live images were taken by a Zeiss inverted microscope (Carl Zeiss, Jena, Germany) equipped with phase-contrast objectives and an AxioCam camera. Live image of beating cells were obtained by a chilled CCD camera (Hamamatsu) using I-O DATA Videorecorder software.

Measurement of Intracellular Ca^{2+} Concentration—Intracellular Ca^{2+} concentration ($[Ca^{2+}]_i$) in beating cells derived from cardiac Sca-1+ cells was measured as previously described (31). The beating cells on gelatin-coated glass coverslips were incubated in HEPES (loading) solution containing 1 μM fluo 3-acetoxymethyl ester (fluo 3-AM; Molecular Probes) at 36 °C in the dark for 30 min. The loading solution was prepared by diluting a 100 μM fluo 3 stock solution, which contained 0.45% Pluronic F127 (Molecular Probes), 10% dimethyl sulfoxide, and 90% FBS. HEPES solution consisted of (in mM) 126 NaCl, 4.4 KCl, 1.0 $MgCl_2$, 1.08 $CaCl_2$, 24 HEPES, 13 NaOH, 11 glucose, and 0.5 probenecid (pH 7.4). The coverslips were washed twice with dye-free HEPES solution and placed in a flow-through chamber on the microscope. Fluo 3-loaded beating cells were excited by 480-nm light and emitted fluorescence was recorded at 530 nm by a photomultiplier tube (AIM-10, InterMedical, Co, Japan) and digitized (PowerLab 2/20, AD-instruments, Castle Hill, Australia). Curve fits were performed with Origin 7J software (MicroCal Software, Northampton, MA). The intensity of the fluorescence at 530 nm increased with an increase in $[Ca^{2+}]_i$.

Estimation of Pluripotency—Osteogenic differentiation of Sca-1+ cells from the adult murine heart was induced in IMDM supplemented with 10% FBS, 50 μM ascorbic acid 2-phosphate, 0.1 μM dexamethasone, and 10

mM β-glycerophosphate as described previously (32). For detection of osteocytes, alkaline phosphatase staining (leukocyte alkaline phosphatase assay kit, Sigma-Aldrich) was used. Adipogenic differentiation was induced as described previously (28). Briefly the cells were cultured with Dulbecco's Modified Eagle's Medium (DMEM) supplemented with 5% horse serum with MDI-I mixture; 0.5 mM methyl-isobutylxanthine, 1 μM dexamethasone, 100 mM indomethacin, and 10 μg/ml insulin for 2 days and then cultured with Dulbecco's modified Eagle's medium supplemented with 5% horse serum and 10 μg/ml of insulin for 1 day. Treatment with MDI-I followed by insulin was repeated four times. For detection of accumulated oil droplets, Oil-Red O staining was performed followed by nuclear hematoxylin counterstaining.

Statistical Analysis—Values are presented as mean ± S.E. The significance of differences among mean values was determined by analysis of variance. The accepted level of significance was $p < 0.05$.

RESULTS

Cell Surface Antigens of Sca-1+ Cells Derived from the Adult Murine Heart—Flow cytometric analysis revealed that Sca-1+ cells were enriched to over 90% when adult murine cardiac cells were sorted twice with the MACS system using PE-conjugated anti-Sca-1 antibody and anti-PE micro beads (Fig. 1*A*). The number of purified Sca-1+ cells was ~1 × 10^4 cells. Limana *et al.* (33) have estimated the number of cardiomyocytes in an adult murine heart as ~3 × 10^6. Therefore the percentage of cardiac Sca-1+ cells was ~0.3% of the total number of cardiomyocytes. Next we examined other cell surface antigens such as CD45, CD34, and c-kit in Sca-1+ cells. After repeated magnetic sorting with biotin-conjugated anti-Sca-1 antibody and anti-biotin micro beads, enriched Sca-1+ cells were incubated with PE-conjugated anti-CD45, CD34 and c-kit antibodies and analyzed by flow cytometry. In enriched Sca-1+ cells, ~40% of the cells expressed CD45 (Fig. 1*B*), and ~10% of the cells expressed CD34 (Fig. 1*C*) and c-kit (Fig. 1*D*).

Sca-1+ Cells from the Adult Murine Heart Differentiate into Beating Cardiomyocytes—In order to induce differentiation into cardiomyocytes, Sca-1+ cells were treated with either 5′-azacytizine or oxytocin. When Sca-1+ cells were cultured with medium containing FBS, they showed various cell shapes, and spindle-like and elongated shapes were predominant (Fig. 2*A*). Two weeks after treatment with oxytocin, small round cells with prominent nucleus and little cytoplasm appeared (*arrowheads* in Fig. 2*B*). These round cells rapidly proliferated, formed clusters, and detached from the culture dish so that spindle-shaped cells were left. The cells were re-plated when reached to confluence. Four weeks after starting treatment with oxytocin, some spontaneously beating cells were recognized among spindle-shaped cells (*arrow* in Fig. 2, *C* and *D* and Supplemental Data). Spontaneous beating was observed at ~1% cells. On the other hand, cells after treatment with 5′-azacytizine or vehicles showed fibroblast-like morphology, and never exhibited round or spindle-shaped morphology, or spontaneous beating.

Next we examined the gene expression of cardiac transcription factors and cardiac structural proteins in Sca-1+ cells by RT-PCR. Before treatment with 5′-azacytizine or oxytocin, only Csx/Nkx-2.5 and GATA4 were slightly expressed (Fig. 3, *lane P*). Four weeks after treatment with 5′-azacytizine or oxytocin, all genes of cardiac transcription factors including Csx/Nkx-2.5, GATA4, and MEF-2C and structural proteins such as α- and β-MHC, MLC-2a, MLC-2v, and cardiac α-actin were expressed (Fig. 3, *lane A* for 5′-azacytizine and *lane OT* for oxytocin). Treatment with 100 nM oxytocin antagonist (OTA, [d(CH_2)$_5$-1,Tyr(Me)-2,Thr-4,Orn-8,Tyr-NH_2-9] vasotocin, Wako, Japan) completely inhibited oxytocin-induced expression of cardiac genes (Fig. 3, *lane OT+OTA*). Total RNA obtained from the adult murine heart and liver were used as positive and negative controls (Fig. 3, *lane H* for heart and *lane L* for liver). Loading of equal amounts of RNA was confirmed by expression of the β-actin gene. Cardiac gene expression was not observed in cells cultured with vehicle (Fig. 3, *lane V*).

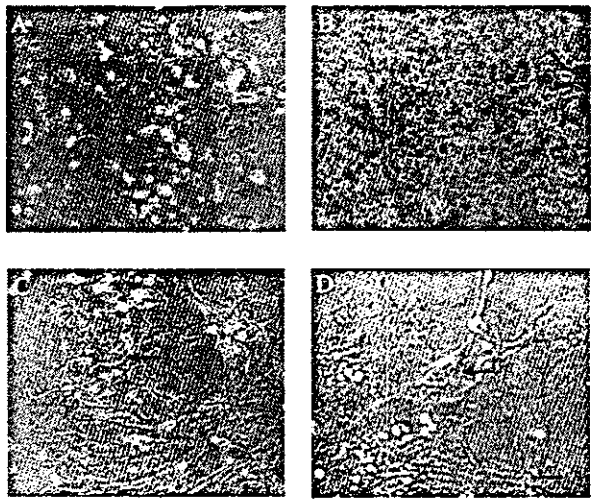

FIG. 2. **Phase contrast images of Sca-1+ cells before and after oxytocin treatment.** *A*, Sca-1+ cells before oxytocin treatment show small spindle-shaped morphology (0 weeks). *B*, two weeks after treatment with oxytocin, small round cells (*arrowheads*) have appeared. These round cells rapidly proliferated, formed clusters, and detached from the culture dish so that spindle-shaped cells were left. The cells were re-plated when reached to confluence. Four weeks after starting treatment with oxytocin, some spontaneously beating cells (*arrow* in *C* and *D*) were recognized among the spindle-shaped cells (*C*). *D*, magnified scale of the figure in *C*. *Bars*, 100 μM.

To examine the expression and localization of cardiac proteins, the Sca-1+ cells treated with oxytocin and 5′-azacytizine were stained with specific antibodies against cardiac proteins. The cells treated with oxytocin expressed GATA4 (Fig. 4*A*), ANF (Fig. 4*B*), and cardiac troponin T (Fig. 4, *A* and *B*). MLC-2v (Fig. 4*C*), sarcomeric myosin heavy chain (Fig. 4*D*), and tropomyosin (data not shown) were also expressed. Notably, staining of each contractile protein showed a fine striated pattern. Connexin 43 was expressed at the junction between two cardiac troponin T-expressing cells (Fig. 4*E*). These findings indicate that treatment with oxytocin induced differentiation of Sca-1+ cells, derived from the adult murine heart, into mature cardiomyocytes, which had well-organized structures and electrical junctions. After treatment with 5′-azacytizine, a fraction of cells expressed sarcomeric myosin heavy chain in fibrillar pattern (Fig. 4*F*), but not cardiac troponin T (data not shown). Next we sorted cardiac Sca-1+ cells on the basis of CD45 expression and cultured with oxytocin. Some of the Sca-1+/CD45− cells expressed sarcomeric myosin after oxytocin treatment, but none of the Sca-1+/CD45+ cells expressed myosin (data not shown), suggesting that Sca-1+ cells that can differentiate into cardiomyocytes are in CD45− population.

Cardiac contraction is regulated by beat to beat change in $[Ca^{2+}]_i$. To ascertain that the spontaneous beating of differentiated cardiac Sca-1+ cells depends on intracellular level of Ca^{2+}, we analyzed $[Ca^{2+}]_i$ transients of the beating cells. As shown in the *upper panel* of Fig. 5*A*, the spontaneous beating of differentiated Sca-1+ cells was accompanied with $[Ca^{2+}]_i$ transients. After treatment with 10^{-7} M isoproterenol for 5 min, the frequency of $[Ca^{2+}]_i$ transients was increased in comparison with control (Fig. 5*A*, *upper panel versus lower panel*). Next we examined the predominant subtype of β receptors, which mediates changes in beating rate. Differentiated cardiac Sca-1+ cells were treated with vehicle (PBS), propranolol, CGP20712A (β_1-selective blocker), or ICI118551 (β_2-selective blocker) for 30

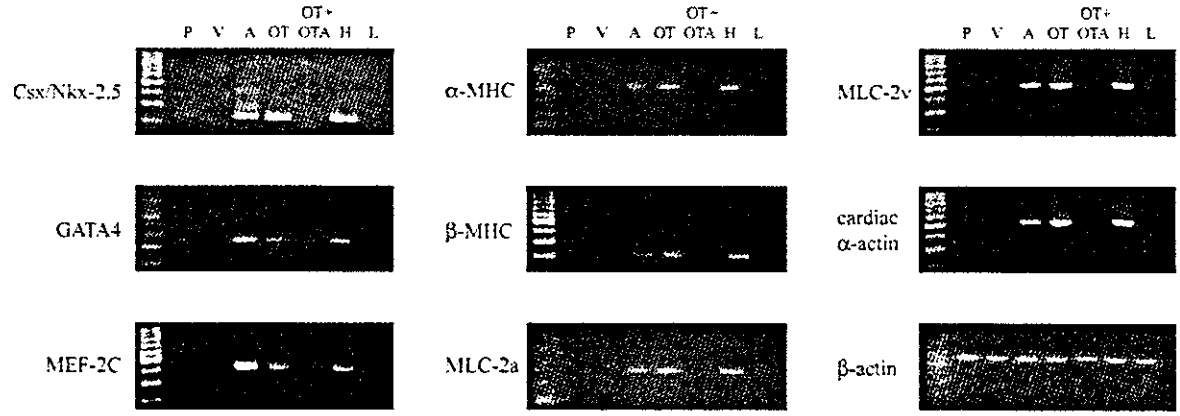

FIG. 3. **RT-PCR analysis of cardiac genes.** Sca-1+ cells after treatment with oxytocin (*lane OT*) or 5'-azacytizine (*lane A*) expressed Csx/Nkx-2.5, GATA4, MEF-2C, α-MHC, β-MHC, MLC-2a, MLC-2v, and cardiac α-actin. Although Sca-1+ cells before treatment (*lane P*) expressed Csx/Nkx-2.5 and GATA4 slightly, none of cells after treatment with vehicles (*lane V*) or oxytocin antagonist combined with oxytocin (*lane OT+OTA*) expressed any cardiac transcription factors. Heart (*lane H*) and liver (*lane L*) were used as positive and negative controls, respectively.

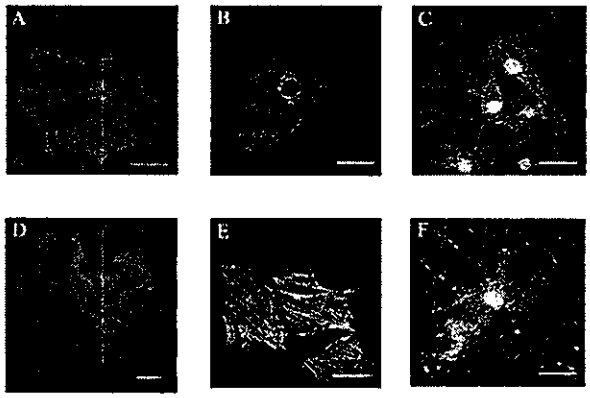

FIG. 4. **Immunocytochemical analysis of cardiac proteins.** *A–E*, cardiac differentiation of Sca-1+ cells after oxytocin treatment. Cells were double-stained using anti-GATA4 antibody (*A*, *green*), anti-ANF antibody (*B*, *green*), and anti-cardiac troponin T antibody (*A* and *B*, *blue*). Cells were stained with anti-MLC-2v (*C*, *green*) and anti-sarcomeric myosin heavy chain antibodies (*D*, *green*), and nuclei were stained with TO-PRO-3 (*C* and *D*, *blue*). Cells were double-stained using anti-cardiac troponin T antibody (*E*, *green*) and anti-connexin 43 antibody (*E*, *blue*). *F*, differentiation of Sca-1+ cells after 5'-azacytizine treatment. Cells were stained with anti-sarcomeric myosin heavy chain (*F*, *green*) and TO-PRO-3 (*F*, *blue*). *Bars*, 50 μm.

min and then stimulated with isoproterenol alone for 5 min. Isoproterenol significantly increased the beating rate of the control cells (control: 131.9 ± 5.6, $n = 10$ *versus* isoproterenol: 228.9 ± 7.3, $n = 10$, $p < 0.01$, Fig. 5*B*). The pretreatment with propranolol (average 196.4 ± 5.6, $n = 10$, $p < 0.05$ *versus* isoproterenol) and CGP20712A (average 188.9 ± 7.5, $n = 10$, $p < 0.05$ *versus* isoproterenol) reduced the increase in beating rate in response to isoproterenol significantly (Fig. 5*B*). ICI118551 had no effect on the isoproterenol-induced increase in beating rate.

Sca-1+ Cells from the Adult Murine Heart Express Oxytocin Receptor mRNA—To elucidate the role of oxytocin receptor in cardiomyogenesis of Sca-1+ cells, we examined the expression of oxytocin receptor in Sca-1+ cells. Oxytocin receptor mRNA was present at low levels in Sca-1+ cells before oxytocin treatment (Fig. 6, *lane P*). Expression levels of oxytocin receptor remained low in cells cultured with vehicle (Fig. 6, *lane V*). After treatment with oxytocin, expression levels of oxytocin receptor were up-regulated (Fig. 6, *lane OT*). In accordance with the inhibitory effect of oxytocin antagonist on oxytocin-induced cardiac differentiation, oxytocin antagonist inhibited oxytocin-induced up-regulation of the oxytocin receptor (Fig. 6, *lane OT+OTA*). These results suggest that the positive feedback mechanism, namely oxytocin-induced up-regulation of oxytocin receptor, plays an important role in oxytocin-induced cardiomyocyte differentiation of cardiac Sca-1+ cells.

Sca-1+ Cells Can Differentiate into Osteocytes and Adipocytes—It has been reported that Sca-1+ cells from skeletal muscle and bone marrow differentiate into various types of cells such as adipocytes, endothelial cells, muscle, neural, and hepatic cells (9, 11, 14). To determine whether the Sca-1+ cells from the adult murine heart have pluripotency, we examined whether these cells could differentiate into cells other than cardiomyocytes. When treated with osteogenic inducers, some of Sca-1+ cells were stained with alkaline phosphatase, one of the early markers of osteogenesis (Fig. 7*A*). RT-PCR clearly revealed that osteogenic marker mRNAs such as alkaline phosphatase and osteocalcin were induced in Sca-1+ cells after treatment with osteogenic inducers (Fig. 7*B*). On the other hand, Sca-1+ cells treated with oxytocin never expressed alkaline phosphatase and osteocalcin. When Sca-1+ cells were cultured with MDI-I mixture for twelve days, some of Sca-1+ cells showed cytoplasmic accumulation of oil droplets stained with Oil-Red O, indicating that Sca-1+ cells differentiated into adipocytes (Fig. 7*C*).

DISCUSSION

In this report, we have first demonstrated that adult cardiac Sca-1+ cells can differentiate into beating cardiomyocytes *in vitro* by treatment with oxytocin. When treated with oxytocin, the Sca-1+ cells expressed cardiac genes including Csx/Nkx-2.5, GATA4, MEF-2C, α-MHC, β-MHC, MLC-2a, MLC-2v, and cardiac α-actin, and cardiac proteins including GATA4, cardiac troponin T, tropomyosin, MLC-2v, sarcomeric myosin heavy chain, ANF, and connexin 43. Furthermore, some of Sca-1+ cells showed well organized sarcomere and spontaneous beating. Although transient treatment with 5'-azacytizine also induced expression of cardiac genes in Sca-1+ cells, it did not induce expression of cardiac troponin T, assembly of sarcomere or spontaneous beating. These results suggest that treatment with 5'-azacytizine induces differentiation of Sca-1+ cells into cardiomyocytes incompletely and that oxytocin is a more potent inducer of cardiac differentiation than 5'-azacytizine.

P19 teratocarcinoma cells differentiate into beating cardiomyocytes after treatment with Me_2SO and have been considered as a good model of *in vitro* cardiogenesis (34, 35). Several

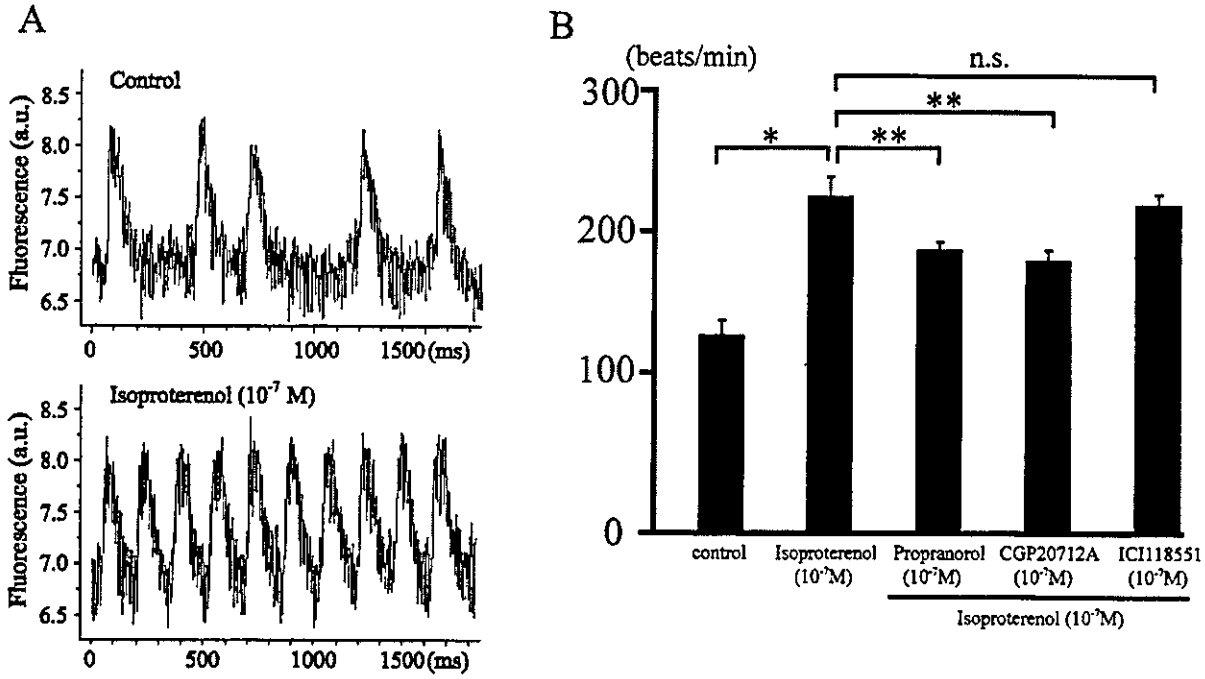

FIG. 5. **Physiological analysis of differentiated cardiac Sca-1+ cells.** *A*, $[Ca^{2+}]_i$ transients of beating cells derived from cardiac Sca-1+ cells before (*upper panel*) and after (*lower panel*) treatment with isoproterenol. *B*, the effects of subtype-specific β receptor blockers on isoproterenol-induced increase in beating rate of differentiated cardiac Sca-1+ cells. Preincubation with 10^{-7} M propranolol (nonselective β blocker) and 10^{-7} M CGP20712A (β_1-selective blocker) reduced isoproterenol-induced increase in beating rate significantly but 10^{-7} M ICI118551 (β_2-selective blocker) did not. *, $p < 0.01$ *versus* control; **, $p < 0.05$ *versus* isoproterenol only; *n.s.*, not significant.

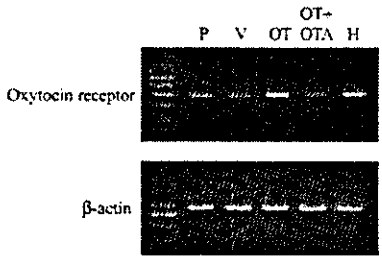

FIG. 6. **RT-PCR analysis of oxytocin receptor expression in Sca-1+ cells.** Oxytocin receptor mRNA was present at low levels in Sca-1+ cells before treatment (*lane P*). After oxytocin treatment, the oxytocin receptor mRNA expression was up-regulated (*lane OT*), but oxytocin antagonist inhibited oxytocin-induced oxytocin receptor up-regulation (*lane OT+OTA*).

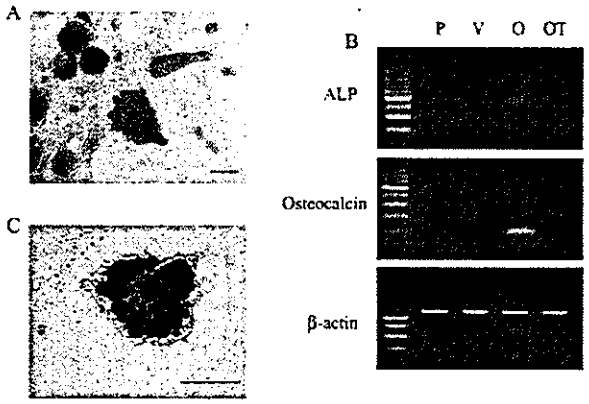

FIG. 7. **Osteogenic and adipogenic differentiation potential of Sca-1+ cells derived from the adult murine heart.** *A*, osteogenic differentiation of Sca-1+ cells was induced by treatment with ascorbic acid 2-phosphate, dexamethasone, and β-glycerophosphate for 3 weeks. Alkaline phosphatase staining (*blue*) was used for detection of osteocytes. *B*, RT-PCR experiment clearly revealed that osteogenic marker mRNAs such as alkaline phosphatase (*ALP*) and osteocalcin were induced in Sca-1+ cells by treatment with osteogenic inducers (*lane P* for pretreatment, *lane V* for vehicle treatment, *lane O* for osteogenic induction). Sca-1+ cells treated with oxytocin never expressed osteogenic marker mRNAs (*lane OT* for oxytocin treatment). β-actin was used as an internal control. *C*, adipogenic differentiation of Sca-1+ cells was induced by treatment with adipogenic mixture (MDI-I) for twelve days. Oil-Red O staining showed adipogenic differentiation of Sca-1+ cells. Hematoxylin was used for counterstaining of nuclei. *Bars*, 50 μm.

essential transcription factors in cardiomyogenesis such as GATA4 (34), Csx/Nkx-2.5 (34), and MEF-2C (36) are up-regulated in P19 cells treated with Me_2SO. Recently Paquin *et al.* (19) have reported that oxytocin induces P19 embryonic carcinoma cells to differentiate into cardiomyocytes. Treatment with oxytocin as well as with Me_2SO induced colony formation of beating cardiomyocytes, expression of cardiac proteins, and oxytocin receptor proteins. In this study, cardiac Sca-1+ cells expressed low levels of oxytocin receptor mRNA that were positively regulated by oxytocin itself, and pretreatment with oxytocin antagonist completely inhibited oxytocin-induced expression of cardiac genes. These results suggest that oxytocin induces cardiomyocyte differentiation of cardiac Sca-1+ cells through oxytocin receptors. Furthermore Sca-1+ cells treated with oxytocin did not express osteogenic marker mRNAs, suggesting that oxytocin is not a nonspecific inducer like 5′-azacytizine but has some specificity for cardiac lineage.

Oxytocin receptors are coupled to $G_{q/11}$ class GTP-binding proteins and stimulate the generation of inositol trisphosphate and diacylglycerol, leading to Ca^{2+} release and activation of protein kinase C (37). Oxytocin stimulates cell proliferation through calcium (38, 39) and protein kinase C pathways (38). Cassoni *et al.* (40) have reported that oxytocin stimulates cell

proliferation through oxytocin receptors that lead to an increase in intracellular Ca^{2+} and tyrosine phosphorylation. Tyrosine phosphorylation in oxytocin signaling has been reported to activate both p38 mitogen-activated protein kinase and extracellular signal-regulated kinase 2 (41, 42). The mechanism by which oxytocin stimulates tyrosine phosphorylation has not been elucidated, but may be mediated by $G\beta\gamma$ subunit dissociating from G_α subunit. Oxytocin inhibits the proliferation of human brain tumors (43), breast cancer cells (44), and adenocarcinoma of endometrium (45) via the cyclic adenosine monophosphate-protein kinase A pathway. Tahara *et al.* (46) have reported that the RhoA/Rho-kinase cascade is involved in oxytocin-induced rat uterine contraction. Among the considerable diversity of oxytocin-mediated signaling pathways, the specific pathway that activates cardiogenesis is currently unknown. Recently post-translational modification of cardiac transcription factors has been reported to be important for their transcriptional activities. Rho-like GTPases can phosphorylate GATA4 via activation of the p38 mitogen-activated protein kinase pathway, which enhances the potency of GATA4 (47). MEF2 is stimulated by calmodulin kinase activation in the heart (48). It remains to be determined which oxytocin signaling pathways are important for differentiation of cardiomyocytes.

It has been reported that c-kit+, Sca-1+, lineage-, and CD34-/low fraction of bone marrow cells contain hematopoietic stem cells, which contribute to long term multilineage reconstitution of the blood system in mice (49). Orlic *et al.* (50) and Gojo *et al.* (10) have reported that c-kit+ bone marrow cells and c-kit+ bone marrow-derived mesenchymal cells transdifferentiate into cardiomyocytes *in vivo*, suggesting that c-kit is one of the cell surface markers of multipotent stem cells in bone marrow. The multipotential stem cells also reside in skeletal muscle, although the origin of the stem cells is still controversial (51). Skeletal muscle-derived stem cells reported by Qu-Petersen *et al.* (11) and Torrente *et al.* (13) highly express CD34 and Sca-1 but not c-kit and CD45 and differentiate into neural and endothelial cells. In our study, cardiac Sca-1+ cells expressed low levels of c-kit, suggesting that the features of stem cell markers on cardiac stem cells is distinct from bone marrow-derived stem cells and rather similar to skeletal muscle-derived stem cells.

Tamaki *et al.* (14) isolated CD34+ and CD45− cells from the interstitial space of skeletal muscle, which highly expressed Sca-1 but not other endothelial progenitor cell markers. The CD34+/CD45− cells differentiated into adipocytes, endothelial and myogenic cells and expressed Bcrp1/ABCG2 gene mRNA, which is an important determinant of the SP phenotype. Recently Polesskaya *et al.* (52) have reported that CD45+/Sca-1+ cells from injured skeletal muscle differentiate into myoblasts much more than CD45−/Sca-1 cells. Because of the hematopoietic restricted expression of CD45 antigen, skeletal myogenic CD45+/Sca-1+ cells might be of hematopoietic origin. In our study, cardiac Sca-1+ cells expressed low levels of CD34 and ~40% of the cardiac Sca-1+ cells expressed CD45, one of hematopoietic cell markers. We sorted cardiac Sca-1+ cells on the basis of CD45 expression and cultured them with oxytocin. Some Sca-1+/CD45− cells expressed sarcomeric myosin after oxytocin treatment, but no Sca-1+/CD45+ cells expressed myosin (data not shown), suggesting that Sca-1+ cells that can differentiate into cardiomyocytes are in the CD45− population. Therefore, in terms of the expression of CD34 and CD45, the cardiac muscle stem cells are distinct from the previously reported skeletal muscle-derived stem cells.

Sca-1+ cells from the adult heart expressed GATA4 and Csx/Nkx-2.5, but not Oct-3/4 before treatment with oxytocin (data not shown), suggesting that the Sca-1+ cells are committed to cardiomyocytes to some degree. Makino *et al.* (24) have reported that mouse bone marrow-derived mesenchymal stem cells (CMG cells) differentiate into cardiomyocyte after 5′-azacytizine treatment. Although the cell surface antigens of CMG cells were not analyzed, the bone marrow-derived mesenchymal stem cells, which differentiated into cardiomyocytes after 5′-azacytizine treatment *in vivo*, expressed Sca-1, c-kit, and CD34 (10), suggesting that the cardiac Sca-1+ cells are different from bone marrow-derived mesenchymal stem cells. Cardiac Sca-1+ cells differentiated into osteocytes and adipocytes in appropriate conditions, suggesting that cardiac Sca-1+ cells have the intragerm layer multipotency. It remains to be determined whether the cardiac Sca-1+ cell population contains stem cells capable of differentiating to extra germ layer lineage.

The spontaneously beating differentiated cardiac Sca-1+ cells showed $[Ca^{2+}]_i$ transients and treatment with isoproterenol increased the frequency of $[Ca^{2+}]_i$ transients and beating rate. The similar response to isoproterenol has been reported in adult murine cardiomyocytes (53), embryonic stem cells-derived cardiomyocytes (54), and CMG cells (55). The β_1-selective blocker, CGP20712A, significantly reduced isoproterenol-induced increase in beating rate to the same extent as the non-selective β-blocker, propranolol, but the β_2-selective blocker, ICI118551, did not. These results suggest that the β_1 receptor is the predominant subtype that mediates the changes in beating rate of cardiomyocytes derived from Sca-1+ cells.

During the preparation of this article, two studies on cardiac stem cells were reported (56, 57). They have shown that c-kit+ or Sca-1+ cells derived from the adult murine heart express cardiac genes and proteins after the cardiogenic induction. We showed for the first time that there are potential adult cardiac stem cells that have an ability to proliferate and differentiate into various types of cells including beating cardiomyocytes *in vitro*. Although the role of cardiac stem cells is uncertain, our results suggest their possible role in cardiac repair. In addition, the understanding of precise molecular mechanisms of the differentiating process of cultured cardiac stem cells may provide us with new insights into cardiac development and regeneration.

Acknowledgments—We thank A. Ohkubo, R. Kobayashi, E. Fujita, M. Watanabe, M. Iida, and Y. Ohtsuki for technical assistance.

REFERENCES

1. Kajstura, J., Leri, A., Finato, N., Di Loreto, C., Beltrami, C. A., and Anversa, P. (1998) *Proc. Natl. Acad. Sci. U. S. A.* **95**, 8801–8805
2. Leri, A., Barlucchi, L., Limana, F., Deptala, A., Darzynkiewicz, Z., Hintze, T. H., Kajstura, J., Nadal-Ginard, B., and Anversa, P. (2001) *Proc. Natl. Acad. Sci. U. S. A.* **98**, 8626–8631
3. Beltrami, A. P., Urbanek, K., Kajstura, J., Yan, S. M., Finato, N., Bussani, R., Nadal-Ginard, B., Silvestri, F., Leri, A., Beltrami, C. A., and Anversa, P. (2001) *N. Eng. J. Med.* **344**, 1750–1757
4. Quaini, F., Urbanek, K., Beltrami, A. P., Finato, N., Beltrami, C. A., Nadal-Ginard, B., Kajstura, J., Leri, A., and Anversa, P. (2002) *N. Eng. J. Med.* **346**, 5–15
5. Anversa, P., and Nadal-Ginard, B. (2002) *Nature* **415**, 240–243
6. Asakura, A., and Rudnicki, M. A. (2002) *Exp. Hematol.* **30**, 1339–1345
7. Hierlihy, A. M., Seale, P., Lobe, C. G., Rudnicki, M. A., and Megeney, L. A. (2002) *FEBS Lett.* **530**, 239–243
8. van der Rijn, M., Heimfeld, S., Spangruade, G. J., and Wiessman, I. L. (1989) *Proc. Natl. Acad. Sci. U. S. A.* **86**, 4634–4638
9. Okumoto, K., Saito, T., Hattori, E., Ito, J. I., Adachi, T., Takeda, T., Sugahara, K., Watanabe, H., Saito, K., Togashi, H., and Kawata, S. (2003) *Biochem. Biophys. Res. Commun.* **304**, 691–695
10. Gojo, S., Gojo, N., Takeda, Y., Mori, T., Abe, H., Kyo, S., Hata, J., and Umezawa, A. (2003) *Exp. Cell Res.* **288**, 51–59
11. Qu-Petersen, Z., Deasy, B., Jankowski, R., Ikezawa, M., Cummins, J., Pruchnic, R., Mytinger, J., Cao, B., Gates, C., Wernig, A., and Huard, J. (2002) *J. Cell Biol.* **157**, 851–864
12. Asakura, A., Seale, P., Girgis-Gabardo, A., and Rudnicki, M. A. (2002) *J. Cell Biol.* **159**, 123–134
13. Torrente, Y., Tremblay, J. P., Pisati, F., Belicchi, M., Rossi, B., Sironi, M., Fortunato, F., El Fahime, M., D'Angelo, M. G., Caron, N. J., Constantin, G., Paulin, D., Scarlato, G., and Bresolin, N. (2001) *J. Cell Biol.* **152**, 335–348

14. Tamaki T., Akatsuka, A., Ando, K., Nakamura, Y., Matsuzawa, H., Hotta, T., Roy, R. R., and Edgerton, V. R. (2002) *J. Cell Biol.* **157,** 571–577
15. Schultheiss, T. M., Burch, J. B., and Lassar, A. B. (1997) *Genes Dev.* **11,** 451–462
16. Sugi, Y., and Lough, J. (1995) *Dev. Biol.* **168,** 567–574
17. Pandur, P., Lasche, M., Eisenberg, L. M., and Kuhl, M. (2002) *Nature* **418,** 636–641
18. Eisenberg, C. A., Gourdie, R. G., and Eisenberg, L. M. (1997) *Development* **124,** 525–536
19. Paquin, J., Danalache, B. A., Jankowski, M., McCann, S. M., and Gutkowska, J. (2002) *Proc. Natl. Acad. Sci. U. S. A.* **99,** 9550–9555
20. Mukaddam-Daher, S., Jankowski, M., Wang, D., Menaouar, A., and Gutkowska, J. (2002) *J. Endocrinol.* **175,** 211–216
21. Yao, A., Kohmoto, O., Oyama, T., Sugishita, Y., Shimizu, T., Harada, K., Matsui, H., Komuro, I., Nagai, R., Matsuo, H., Serizawa, T., Maruyama, T., and Takahashi, T. (2003) *Circ. J.* **67,** 83–90
22. Komuro, I., and Izumo, S. (1993) *Proc. Natl. Acad. Sci. U. S. A.* **90,** 8145–8149
23. Brunskill, E. W., Witte, D. P., Yutzey, K. E., and Potter, S. S. (2001) *Dev. Biol.* **235,** 507–520
24. Swanson, B. J., Jack, H. M., and Lyons, G. E. (1998) *Mol. Immunol.* **35,** 445–458
25. Robbins, J., Gulick, J., Sanchez, A., Howles, P., and Doetschman, T. (1990) *J. Biol. Chem.* **265,** 11905–11909
26. Kubalak, S. W., Miller-Hance, W. C., O'Brien, T. X., Dyson, E., and Chien, K. R. (1994) *J. Biol. Chem.* **269,** 16961–16970
27. Makino, S., Fukuda, K., Miyoshi, S., Konishi, F., Kodama, H., Pan, J., Sano, M., Takahashi, T., Hori, S., Abe, H., Hata, J., Umezawa, A., and Ogawa, S. (1999) *J. Clin. Investig.* **103,** 697–705
28. Asakura, A., Komaki, M., and Rudnicki, M. A. (2001) *Differentiation* **68,** 245–253
29. Zur Nieden, N. I., Kempka, G., and Ahr, H. J. (2002) *Differentiation* **71,** 18–27
30. Bi, W., Drake, C. J., and Schwarz, J. J. (1999) *Dev. Biol.* **211,** 255–267
31. Yao, A., Su, Z., Nonaka, A., Zubair, I., Spitzer, K. W., Bridge, J. H., Muelheims, G., Ross, J. Jr., and Barry, W. H. (1998) *Am. J. Physiol.* **275,** H1441-H1448
32. Jaiswal, N., Haynesworth, S. E., Caplan, A. I., and Bruder, S. P. (1997) *J. Cell Biochem.* **64,** 295–312
33. Limana, F., Urbanek, K., Chimenti, S., Quaini, F., Leri, A., Kajstura, J., Nadal-Ginard, B., Izumo, S., and Anversa, P. (2002) *Proc. Natl. Acad. Sci. U. S. A.* **99,** 6257–6262
34. Monzen, K., Shiojima, I., Hiroi, Y., Kudoh, S., Oka, T., Takimoto, E., Hayashi, D., Hosoda, T., Habara-Ohkubo, A., Nakaoka, T., Fujita, T., Yazaki, Y., and Komuro, I. (1999) *Mol. Cell. Biol.* **19,** 1096–1105
35. Hiroi, Y., Kudoh, S., Monzen, K., Ikeda, Y., Yazaki, Y., Nagai, R., and Komuro, I. (2001) *Nat. Genet.* **28,** 276–280
36. Skerjanc, I. S., Petropoulos, H., Ridgeway, A. G., and Wilton, S. (1998) *J. Biol. Chem.* **273,** 34904–34910
37. Hoare, S., Copland, J., Strakova, Z., Ives, K., Jeng, Y. J., Hellmich, M. R., and Soloff, M. S. (1999) *J. Biol. Chem.* **274,** 28682–28689
38. Thibonnier, M., Conarty, D. M., Preston, J. A., Plesnicher, C. L., Dweik, R. A., and Erzurum, S. C. (1999) *Endocrinology* **140,** 1301–1309
39. Tahara, A., Tsukada, J., Tomura, Y., Wada, K., Kusayama, T., Ishii, N., Yatsu, T., Uchida, W., and Tanaka, A. (2000) *Br. J. Pharmacol.* **129,** 131–139
40. Cassoni, P., Sapino, A., Munaron, L., Deaglio, S., Chini, B., Graziani, A., Ahmed, A., and Bussolati, G. (2001) *Endocrinology* **142,** 1130–1136
41. Ohmichi, M., Koike, K., Nohara, A., Kanda, Y., Sakamoto, Y., Zhang, Z. X., Hirota, K., and Miyake, A. (1995) *Endocrinology* **136,** 2082–2087
42. Strakova, Z., Copland, J. A., Lolait, S. J., and Soloff, M. S. (1998) *Am. J. Physiol.* **274,** E634–641
43. Cassoni, P., Sapino, A., Stella, A., Fortunati, N., and Bussolati, G. (1998) *Int. J. Cancer* **77,** 695–700
44. Cassoni, P., Fulcheri, E., Carcangiu, M. L., Stella, A., Deaglio, S., and Bussolati, G. (2000) *J. Pathol.* **190,** 470–477
45. Cassoni, P., Sapino, A., Fortunati, N., Munaron, L., Chini, B., and Bussolati, G. (1997) *Int. J. Cancer* **72,** 340–344
46. Tahara, M., Morishige, K., Sawada, K., Ikebuchi, Y., Kawagishi, R., Tasaka, K., and Murata, Y. (2002) *Endocrininology* **143,** 920–929
47. Wei, L., Roberts, W., Wang, L., Yamada, M., Zhang, S., Zhao, Z., Rivkees, S. A., Schwartz, R. J., and Imanaka-Yoshida, K. (2001) *Development* **128,** 2953–2962
48. Passier, R., Zeng, H., Frey, N., Naya, F. J., Nicol, R. L., McKinsey, T. A., Overbeek, P., Richardson, J. A., Grant, S. R., and Olson, E. N. (2000) *J. Clin. Investig.* **105,** 1395–1406
49. Osawa, M., Hanada, K., Hamada, H., and Nakauchi, H. (1996) *Science* **273,** 242–245
50. Orlic, D., Kajstura, J., Chimenti, S., Jakoniuk, I., Anderson, S. M., Li, B., Pickel, J., Mckay, R., Nadal-Ginard, B., Bodine, D. M., Leri, A., and Anversa, P. (2001) *Nature* **410,** 701–705
51. McKinney-Freeman, S. L., Jackson, K. A., Camargo, F. D., Ferrari, G., Mavilio, F., and Goodell, M. A. (2002) *Proc. Natl. Acad. Sci. U. S. A.* **99,** 1341–1346
52. Polesskaya, A., Seale, P., and Rudnicki, M. A. (2003) *Cell* **113,** 841–852
53. Lu, S., Hoey, A. (1998) *J. Mol. Cell Cardiol.* **32,** 143–152
54. Wobus, A. M., Wallukat, G., and Hescheler, J. (1991) *Differentiation* **48,** 173–182
55. Hakuno, D., Fukuda, K., Makino, S., Konishi, F., Tomita, Y., Manabe, T., Suzuki, Y., Umezawa, A., and Ogawa, S. (2002) *Circulation* **105,** 380–386
56. Beltrami, A. P., Barlucchi, L., Torella, D., Baker, M., Limana, F., Chimenti, S., Kasahara, H., Rota, M., Musso, E., Urbanek, K., Leri, A., Kajstura, J., Nadal-Ginard, B., and Anversa, P. (2003) *Cell* **114,** 763–776
57. Oh, H., Bradfute, S. B., Gallardo, T. D., Nakamura, T., Gaussin, V., Mishina, Y., Pocius, J., Michael, L. H., Behringer, R. R., Garry, D. J., Entman, M. L., and Schneider, M. D. (2003) *Proc. Natl. Acad. Sci. U. S. A.* **100,** 12313–12318

Human Molecular Genetics, 2004, Vol. 13, No. 2 *151–157*
DOI: 10.1093/hmg/ddh014
Advance Access published on November 25, 2003

Overexpression of P104L mutant caveolin-3 in mice develops hypertrophic cardiomyopathy with enhanced contractility in association with increased endothelial nitric oxide synthase activity

Yutaka Ohsawa[1], Haruhiro Toko[2], Masashi Katsura[3], Kazue Morimoto[1], Haruki Yamada[1], Yaeko Ichikawa[1], Tatsufumi Murakami[1], Seitaro Ohkuma[3], Issei Komuro[2] and Yoshihide Sunada[1,*]

[1]Division of Neurology, Department of Internal Medicine, Kawasaki Medical School, 577 Matsushima, Kurashiki-City, Okayama 701-0192, Japan, [2]Department of Cardiovascular Science and Medicine, Chiba University Graduate School of Medicine, 1-8-1 Inohana, Chuo-ku, Chiba 260-8670, Japan and [3]Department of Pharmacology, Kawasaki Medical School, 577 Matsushima, Kurashiki-City, Okayama 701-0192, Japan

Received July 8, 2003; Revised and Accepted November 11, 2003

The effect of endogenous nitric oxide synthase (NOS) on cardiac contractility and architecture has been a matter of debate. A role for NOS in cardiac hypertrophy has recently been demonstrated by studies which have shown hypertrophic cardiomyopathy (HCM) with altered contractility in constitutive NOS (cNOS) knockout mice. Caveolin-3, a strong inhibitor of all NOS isoforms, is expressed in sarcolemmal caveolae microdomains and binds to cNOS *in vivo*: endothelial nitric oxide synthase (eNOS) in cardiac myocytes and neuronal nitric oxide synthase (nNOS) in skeletal myocytes. The current study characterized the biochemical and cardiac parameters of P104L mutant caveolin-3 transgenic mice, a model of an autosomal dominant limb-girdle muscular dystrophy (LGMD1C). Transgenic mouse hearts demonstrated HCM, enhanced basal contractility, decreased left ventricular end diastolic diameter, and loss and cytoplasmic mislocalization of caveolin-3 protein. Surprisingly, cardiac muscle showed activation of eNOS catalytic activity without increased expression of all NOS isoforms. These data suggest that a moderate increase in eNOS activity associated with loss of caveolin-3 results in HCM.

INTRODUCTION

Caveolae are 50–100 nm flask-shaped invaginations of the plasma membrane that are primarily composed of the 21–24 kDa integral membrane proteins, caveolin-1, -2 and -3 (1). These structures participate in vesicular trafficking events and signal transduction by acting as scaffold proteins for specific lipids and lipid-modified signaling molecules (e.g. cholesterol, G-proteins, G-protein coupled receptors, receptor tyrosine kinases and nitric oxide synthase) (2–4).

Caveolin-3 is a myocyte-specific isoform that assembles to ~350 kDa homo-oligomers in the sarcoplasmic reticulum (SR) (2). Caveolin-3 homo-oligomers are translocated to the plasma membrane via the trans-Golgi network (2,4) and inhibit all NOS isoforms *in vitro* and bind to constitutive NOS (cNOS) *in vivo*: endothelial nitric oxide synthase (eNOS) in cardiac myocytes and neuronal nitric oxide synthase (nNOS) in skeletal myocytes (5–8).

Autosomal dominant limb-girdle muscular dystrophy 1C (LGMD1C) and autosomal dominant rippling muscle disease (AD-RMD) result from heterozygous mutations of the skeletal muscle caveolin-3 gene (*CAV3*) (9,10). We previously generated transgenic (Tg) mice (TgCAV3M1 mice) with severe myopathy secondary to overexpression of P104L mutant caveolin-3 as a model of LGMD1C (11). Further study of this transgenic animal model revealed increased sarcolemmal nNOS activity without alternations of nNOS expression at both mRNA and protein levels. Other reports demonstrated that caveolin-3 is down-regulated in the hypertrophic hearts of spontaneously hypertensive rats (12) and that circulatory NO

*To whom correspondence should be addressed: Tel: +81 864621111; Fax: +81 864621199; Email: ysunada@med.kawasaki-m.ac.jp

(13) or eNOS mRNA in cardiac muscle (14) increases in human heart failure. These observations suggest that loss of caveolin-3 may modulate cardiac architecture and function via disinhibition of NOS activity. The present study investigated this hypothesis by characterizing the biochemical and cardiac parameters of TgCAV3M1 mice.

RESULTS

TgCAV3M1 mice show hypertrophic cardiomyopathy with enhanced contractility

TgCAV3M1 mice were generated as described previously (11). Tg mice showed poor growth and were significantly smaller than their wild-type (Wt) littermates at 4, 12, 24 and 36 weeks of age (Fig. 1A) and demonstrated kyphosis of the spine and paralysis of the hindlimbs from 12 weeks of age. The Tg mice exhibited increased cardiac weight and statistically significant increases in the cardiac weight-to-body weight ratio at 4, 12, 24 and 36 weeks of age when compared with their Wt littermates (Fig. 1B and C). However, from the clinical standpoint, the Tg mice have so far not developed any significant symptoms of heart failure, nor have any significant differences in life span been observed between the Wt and Tg mice.

Gross appearance of the hearts from 6-week-old Wt and Tg mice at the lower ventricular level showed thickening of the interventricular septum and the posterior wall of the left ventricle, resulting in a smaller left ventricular chamber in the Tg mice (Fig. 2A). Hematoxylin and eosin staining of cardiac muscle sections showed hypertrophy of cardiac myofibers in the Tg mice (Fig. 2B). The diameters of 1000 cardiac muscle fibers from five Tg mice and five Wt mice, respectively, were measured. The frequency distribution (percentage) of the cardiac myofiber diameter in Tg mice showed a distribution skew to the right and marked size variability on both longitudinal and transverse sections when compared to Wt mice (Fig. 2C). The mean cardiac muscle fiber diameter and standard deviation were significantly larger ($P < 0.05$) in Tg mice (8.53 ± 1.43 μm on longitudinal section and 9.35 ± 1.17 μm on transverse sections) than in Wt mice (6.55 ± 0.91 and 7.32 ± 0.83 μm, respectively; Fig. 2C). Gene expression of cardiac myocyte hypertrophic markers, atrial natriuretic peptide (ANP) and brain-derived natriuretic peptide (BNP) was analyzed by northern blotting. Densitometry using BAS2000 Image Analyzer demonstrated that both the ANP and BNP transcripts in the Tg mouse hearts were up-regulated by 1.69- and 1.54-fold, respectively (Fig. 2D). Transthoracic echocardiogram performed in 24-week-old Tg mice ($n = 7$) revealed unique pathophysiological characteristics for HCM; increased thickness of the interventricular septum and left ventricular posterior wall, hypercontractility (increased left ventricular fractional shortening) and diastolic dysfunction (decreased left ventricular end diastolic diameter; Table 1).

Tg CAV3M1 mouse hearts show loss and cytoplasmic mislocalization of caveolin-3

Northern blot analysis of Tg mouse cardiac muscle showed overexpression of smaller-sized (~1.1 kb) mutant caveolin-3 mRNA (Fig. 3A). Detection of endogenous caveolin-3 mRNA (~1.4 kb) in the Tg mice was interfered with by an excessive amount of the mutant caveolin-3 mRNA. Then, the differential expression of endogenous and mutant caveolin-3 mRNA was analyzed by RT–PCR using two distinct reverse primers as described previously (11). RT–PCR confirmed the expression of endogenous caveolin-3 mRNA in Tg mouse hearts as well as in Wt mouse hearts, as shown in Figure 3B.

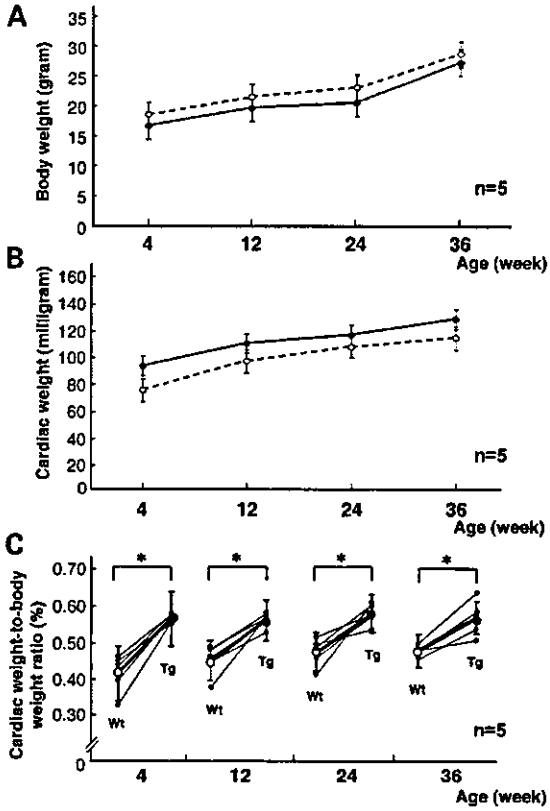

Figure 1. Comparison of body weight (**A**), cardiac weight (**B**) and the cardiac weight-to-body weight ratio (**C**) between Wt (open circle, $n = 5$) and Tg (solid circle, $n = 5$) mice at 4, 12, 24 and 36 weeks of age. Note that the smaller body weight and larger cardiac weight in the Tg mice results in statistically significant increases in the mean cardiac weight-to-body weight ratios. Error bars are ±SD. *Statistical significance was determined by *Welch's t*-test ($P < 0.05$).

In sharp contrast to overexpression of mutant caveolin-3 mRNA, immunoblot analysis showed a marked reduction (~95%) of caveolin-3 protein in Tg mouse cardiac muscle (Fig. 3C). Immunohistochemical analysis demonstrated sarcolemmal localization of caveolin-3 protein in the Wt mice, while the majority of cardiac muscle fibers of the Tg mice showed only weak sarcolemmal immunoreactivity with small, cytoplasmic, dot-like immunoreactivity (Fig. 3D). There was no change in sarcolemmal dystrophin expression in the Tg mice (Fig. 3D). Caveolin-1 was expressed in endothelial cells and showed no compensatory overexpression in Tg mouse cardiac myocytes (Fig. 3D). β-Dystroglycan expression was similar in the Wt and Tg mice (Fig. 3C).